



Parameters extraction of three diode photovoltaic models using boosted LSHADE algorithm and Newton Raphson method

Hussein Mohammed Ridha ^{a, b}, Hashim Hizam ^{a, b, *}, Chandima Gomes ^c, Ali Asghar Heidari ^{d, e, 1}, Huiling Chen ^{f, **}, Masoud Ahmadipour ^{a, b}, Dhiaa Halboot Muhsen ^g, Mokhalad Alghrairi ^{a, h}

^a Department of Electrical and Electronics Engineering, Faculty of Engineering, Universiti Putra Malaysia, 43400, Serdang, Malaysia

^b Advanced Lightning, Power and Energy Research (ALPER), Faculty of Engineering, Universiti Putra Malaysia, 43400, Serdang, Malaysia

^c School of Electrical and Information Engineering, University of Witwatersrand, 1 Jan Smuts Avenue, Braamfontein, Johannesburg, 2000, South Africa

^d School of Surveying and Geospatial Engineering, College of Engineering, University of Tehran, Tehran, Iran

^e Department of Computer Science, School of Computing, National University of Singapore, Singapore

^f Department of Computer Science and Artificial Intelligence, Wenzhou University, Wenzhou, 325035, China

^g Department of Computer Engineering, University of Al-Mustansiriyah, 10001, Baghdad Iraq

^h Department of Computer Techniques Engineering, Imam Al Kadhim College (IKC), 10087, Baghdad, Iraq

ARTICLE INFO

Article history:

Received 26 September 2020

Received in revised form

23 January 2021

Accepted 13 February 2021

Available online 18 February 2021

Keywords:

Parameters extraction

Photovoltaic model

Differential evolution

Newton raphson method

Lambert W function

ABSTRACT

The (photovoltaic) PV models' performance is strongly dependent on their parameters, which are mainly standing on the utilized method and the formulated objective function. Therefore, extracting the PV models' parameters under several environmental conditions is crucial for maximizing its reliability, accuracy and reducing the system's overall cost. According to the scope of this problem, several methodologies have been extensively applied to tackle this problem. Thus, this paper presents an enhanced version of the well-known LSHADE (ELSHADE) method by integrating various contributions in the algorithm itself and the objective function to determine three diode PV models' parameters. In ELSHADE, the population is divided into two phases: a robust mutation scheme performs the first phase, and the chaotic-guided strategy is utilized in the second stage. Moreover, an improved Newton Raphson (INR) method is presented to address the I–V curve equation's chaotic behavior effectively. The results confirm that the proposed ELSHADE-INR can precisely find the global solutions by comparing it with state-of-the-art algorithms and its superiority demonstrated in several statistical criteria under real experimental data. The average values of root mean square error (RMSE), mean bias error, determination coefficient, deviation of RMSE, test statistical, absolute error, and CPU-execution time are 0.0060 and 5.88e-05, 0.9999, 2.54e-05, 0.0538, and 0.0042, 11.39s, respectively. We observed that the proposed ELSHADE is robust and stable, and very promising in its origin to obtain high-quality and accurate parameters. This paper is supported by <https://aliasgharheidari.com/publications/ELSHADE.html>.

© 2021 Elsevier Ltd. All rights reserved.

1. Introduction

In the last decades, the development of renewable energy applications has been significantly boosted [1]. This is due to the rapid depletion of conventional energy sources [89] and their side effects [90], such as pollution [2,92,93], reduction in the price of renewable energy sources [91], and permanently ubiquitous in nature [3]. In particular, the solar photovoltaic (PV) system [4,88] is one of the most promising sources of renewable energy sources, with more than 115 GW of the solar PV systems from 200 GW added in 2019 [5]. They can be installed anywhere and support future cities for the

* Corresponding author. Department of Electrical and Electronics Engineering, Faculty of Engineering, Universiti Putra Malaysia, 43400, Serdang, Malaysia.

** Corresponding author. Department of Computer Science and Artificial Intelligence, Wenzhou University, Wenzhou, 325035, China.

E-mail addresses: hussain_mhammad@yahoo.com (H.M. Ridha), hhizam@upm.edu.my (H. Hizam), chandima.gomes@wits.ac.za (C. Gomes), as_heidari@ut.ac.ir, aliasgha@comp.nus.edu.sg, t0917038@u.nus.edu (A.A. Heidari), chenhuiying.jlu@gmail.com (H. Chen), maseod.ahmadipour@gmail.com (M. Ahmadipour), deia_mohussen@yahoo.com (D.H. Muhsen), mokhalad.khalel@alkadum-col.edu.iq (M. Alghrairi).

¹ <https://aliasgharheidari.com>

best level of energy supply. However, there is no perfection in the industry, and several new challenges and problems appear with the new technologies in PV systems. Despite the exponential growth in the solar PV system, several factors may limit its separation, such as solar irradiance, high initial costs, and low energy conversion [6,7].

From a previous point of view, it is crucial to utilize an accurate and reliable PV model to describe the PV system's actual behavior under various weather conditions [8]. The PV model's performance can be verified by correctly forecasting the I–V and P–V curves, as well as statistical criteria analysis [9,10]. Essentially, there are three standard electrical PV circuits: single-diode (SD) PV model, double-diode (DD) PV model, and the three-diode (TD) model. The simplest one is the SD PV model, while the DD PV model is preferred at low solar irradiance. However, the TD PV model can factually correct the SD and DD PV models' imperfections by representing the leakage current in the grain regions of the multi-crystalline silicon solar cells [11]. Therefore, the main aim of proposing the TD PV model is to be utilized for industrial applications [12]. At a rough guess, the parameters of the PV cell/module can be extracted either by using three key points on the I–V curve, which are usually given by the manufacturer at standard test conditions (STC) such as an open circuit (OC), short-circuit (SC), and maximum power point (MPP) [13], or by minimizing the error between the simulated and experimental currents [14,15]. In fact, the curve-fitting methods based on actual laboratory environmental conditions are considered more adequate and reflect the PV cells' realistic performance. Bearing in mind, the experimental data can contain many errors and noises during the measurement [16].

Based on the literature, a variety of approaches have been extensively employed to solve the parameters extraction optimization problem, such as numerical, Newton Raphson (NR) [17], tabular [3], and curve-fitting method [18]. The advantages of numerical methods are presumed to be accurate if the initial state of the parameters is chosen carefully, especially when the optimization problem is high-dimensional and multi-model [19]. In contrast, these methods' significant obstacles are: they require a prolonged execution time. Their output can deteriorate when the number of the parameters that need to be extracted is large [20]. The second category of the extraction parameter methods is mathematical algebraic equations, which usually convert and approximate the equations into a simple and explicit form based on the critical points on the I–V data curve [21]. The analytical methods also provide fast calculations for resolving the nonlinear and multi-model equations to extract the PV cell/module parameters [22]. However, predicting the parameters based on analytical methods has several negative consequences. The parameters are estimated based on datasheet information at STC, which frequently do not represent the PV system's natural behavior [23,24]. Hence, such an optimization problem has several local minima and multivariable. In comparison, these methods do not consider noise-effect [25]. Another aspect is the estimated I–V curve based on datasheet information, mostly in ideal representations where the voltage values are figured out utilizing linear assumptions [26]. Also, intense computing is challenging and essential to extract the parameters of the three diode PV model [27]. To bring an end to this, the values of the parameters are changeable during the day. They are location-dependent, while these methods can neither evaluate all the parameters' variations nor match the actual performance using the shifted equations [28–31].

Optimization methods are trendy and not limited to single objective optimizers. Any single objective case can be extended to more forms of the cases such as robust optimization [32], hybrid methods [33], multiobjective cases [97], many objective approaches [98,99], fuzzy optimization [100], and large scale techniques [34]. There are some population-based optimizers, such as

applications of differential search (DS) [35], differential evolution (DE) [36], particle swarm optimizer (PSO) [37], teaching-learning-based optimizer (TLBO) [38], and whale optimizer (WOA) [39], known as nature-inspired and evolutionary methods, as an alternative way to the deterministic methods (or beside them). The most trusted methods are those with a strong evolutionary basis and with a language free of metaphor.

Meta-heuristic methods have been extensively employed in the last decades to address parameter extraction optimization [40,41]. This is because these methods can provide the potential to overcome the shortcomings of numerical and analytical methods. Besides, the solutions-quality is significantly enhanced by using the intensification and diversification techniques and the effectiveness of tackling the problem of initial conditions [42]. Moreover, the parameter extraction optimization problem can be optimally formulated by using statistical criteria such as Root Mean Square Error (RMSE) and Absolute Error (AE), which can reduce the execution time and error between the experimental and proposed currents [43]. Finally, the nonlinearity and noise effects can somehow be limited by these methods [44]. Despite all the benefits of the meta-heuristic methods, there are some weaknesses: in high-dimensional PV models, they can be easily trapped in local minima, and the possible parameters' setting should be tuned carefully [45]. The exploration and exploitation phases can hardly be harmonized in dealing with the TD PV model due to the broad variables in which the degradation can be observed in accuracy.

For the reason of the above limitations of the basic meta-heuristic methods, the hybrid and enhanced methods are produced. They can officially attain a higher degree of precision by merging two or more than one operators to achieve satisfactory results [46]. These kinds of methods have a higher potential to excel and discover more new areas and enrich solutions quality. Consequently, the development of these improved methods is complicated as they need us to put more effort into the optimization problem, programming, noise effects, and statistics. There are several well-published research papers based on hybrid and enhanced methods. Examples are teaching-learning based on performance-guided JAYA algorithm (PGJAYA) [8], onlooker-ranking based on adaptive DE (ORcr-IJADE) [47], linear population size reduction based on success history adaptive DE (LSHADE) [48], multi-strategy LSHADE (MLSHADE) [49], multiple learning BSA (MLBSA) [50], and etc. The other enhanced and hybrid methods cannot be covered due to a considerable number of published papers. The subject of the estimation of the parameters optimization problem of the PV model is an ongoing topic. However, readers can refer to a recent review of utilized methods for PV models [40,51].

Despite a large number of articles that have been developed in the literature, due to the rapid evolution of the PV module and the progress in its efficiency in particular with involving the bifacial PV technology [52], there is still a theoretical gap in finding global solutions under all weather conditions. This is attributed to the complexity, lack of experimental data at different weather conditions, and unpredictable behavior of the PV model equation. Unfortunately, much of the studies still calculate the PV cell's current directly without considering its nonlinearity or variety of each parameter [49], resulting in an undesirable level of accuracy [53]. To solve this dilemma, many methods have been implemented to effectively deal with electrical circuit equations, such as the Taylor series [54], f-solve command built-in MATLAB software [48], NR method [55,56], and Lambert W function [57–59]. However, the TS method's key downside is that it takes a longer time and less convergence than the NR method [60]. The NR method has a rapid convergence, which results in less AE. Simultaneously, the Lambert W function takes more CPU-execution time analog with better accuracy, especially at a high voltage level. Therefore, the

challenges are to achieve a balance between the exploration and exploitation phases and that it is indispensable to maintain better stability and accuracy. Concerning the above, Yousri et al. [61] compared many optimizers and methods to extract parameters of the SD, DD, TD PV models using RMSE as an objective function via the NR method and direct linear PV model equation method. Whilst, the Lambert W function method is employed to identify which method has better accuracy. The experimental results improved that one of the recent methods based on the NR method has superiority in accuracy and fast convergence than other literature procedures. However, no attention was given to the TD PV model's parameter extraction based on the Lambert W function.

According to the literature, the differential evolution (DE) method has speedy developments and improvements because it is powerful, flexible, and sufficient, reliable enough to deal with various types of optimization problems [62–65]. Therefore, Biswas et al. combined analytical and LSHADE methods to extract the SD and DD PV models' parameters based on three critical points from datasheet information [48]. I_0 and I_{ph} were mathematically extracted. Then, d , R_s , and R_p were optimally determined by using LSHADE method. The objective function was formulated by minimizing the summation of errors between the main three reference points. Subsequently, the best I–V curve was plotted by considering all optimal solutions based on the f-solve command. One of the major obstacles of the proposed method is by plotting the I–V curve based on only the datasheet information which is insufficient for actual performance. Afterward, MLSHADE was proposed to solve the parameters identification of the SD and DD PV cell/module [49]. The novelty of MLSHADE was achieved by a weighted mutation strategy and inferior solutions search of enriching exploration capability and local minima avoidance in the first phase. In the second phase, Eigen Gaussian random walk mechanism was employed for better performance. Despite all efforts to improve the MLSHADE algorithm, the PV model equation was linearly resolved. Another was conducted using an improved version of the JAYA algorithm for parameter extraction of the SD and DD PV cell/module [8]. In the PGJAYA algorithm, each individual, based on probability, was self-adapted to select a different evolution strategy. Additionally, the quantified performance was used for improving the search direction. Finally, a disorderly disturbance tactic was used to discover new search regions. From the experimental findings, PGJAYA was able to exceed a variety of well-regard algorithms. With similar goals, MLBSA was proposed to find optimal parameters of the SD and DD PV cell/module [50]. In MLBSA, some individuals were addressed to learn from the historical and current population simultaneously. On the other hand, the rest individuals were learned from the current and best solutions. Also, a chaotic local search (CLS) mechanism was utilized to enrich diversity ability. However, a linear PV model equation was obtained to predict the works' output current [8,50]. The authors of [66] combined chaotic logistic sequence with Rao-1 algorithm to extract the PV cell/module parameters under real experimental data. The performance results of the LCROA validated by comparing it with well-known algorithms. While Ridha et al. [67] employed Marine Predators Algorithm to extract the SD and DD PV model parameters under various real weather conditions. The equation of the PV model was solved by utilizing the Lambert W function. The MPALW method outperformed several well-published methods and showed a good agreement with experimental data especially at high voltage ranges. To end this, the MRFO is a new meta-heuristic that was considered by Ref. [68] to extract the parameters of the TD PV model using nameplate datasheet information.

Based on the authors' knowledge, no up to date method can be stated that the optimum parameters extracted are global solutions. Therefore, finding a reliable, accurate, efficient, and stable

algorithm is necessary to meet the PV system's actual performance under any weather conditions. The following highlights summarize the main contribution of this paper:

- A novel ELSHADE-INR method is developed to extract the parameters of the TD PV model optimally.
- Efficient population classification based on mutation and guided-chaotic strategies is proposed to enrich the exploitation ability and increase the population's diversity.
- An improved NR method is proposed using damping to mimic the PV model's equation's nonlinearity behavior and large iterations avoidance. This idea is designed to result in an excellent initial estimation of the root significantly.
- The proposed method's performance is verified by utilizing real experimental data under different environmental conditions and compared with well-regard methods.
- The ELSHADE-INR method outperformed two variants of the LSHADE method referred to as ELSHADE-LW and ELSHADE based on the Lambert W function and NR methods, respectively.

2. Photovoltaic models and objective function

2.1. Three diode PV model

The three diode PV model's electrical equivalent circuit is illustrated in Fig. 1. In general, there are nine physical parameters comprised TD PV model: a current source I_{ph} in (A) connected in parallel, diodes ideality factor d_1 , d_2 , and d_3 connected in the opposite direction to reflect the output voltage of the PV cells, the saturation currents of the diode I_{o1} , I_{o2} , and I_{o3} in (A), large shunt resistance R_p in (Ω) connected in parallel to describe the diode's saturation current, and small series resistance R_s in (Ω). The output current I in (A) of the PV cell can be computed by using Kirchhoff's law and defined by,

$$I = I_{ph} - I_d - I_p \quad (1)$$

where I_d is the forward diode current in (A) and I_p is the shunt resistor current in (A). Thus, I_d can be calculated by utilizing the Shockley diode law as follows:

$$I_d = I_{o1} \left[\exp\left(\frac{V + IR_s}{V_{t1}}\right) - 1 \right] - I_{o2} \left[\exp\left(\frac{V + IR_s}{V_{t2}}\right) - 1 \right] - I_{o3} \left[\exp\left(\frac{V + IR_s}{V_{t3}}\right) - 1 \right] \quad (2)$$

where V refers to the output voltage (V) and $V_{t1} - V_{t3}$ are the diode's thermal voltage (V) and can be written by the following:

$$V_{t1} = \frac{d_1 K B T_c}{q} V_{t2} = \frac{d_2 K B T_c}{q} V_{t3} = \frac{d_3 K B T_c}{q} \quad (3)$$

where $K B$ represents the constant of Boltzmann ($1.38 \times 10^{-23} J/K$),

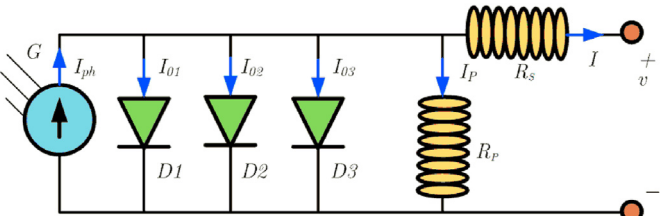


Fig. 1. The electrical circuit of the TD PV model.

T_c is the cell temperature (K), and q is the electron charge ($1.60 \times 10^{-19} C$). The I_p can be given as follows:

$$I_p = \frac{V + IR_s}{R_p} \quad (4)$$

Hence, by solving Eqs. (1)–(4), the I is represented by the following equation:

$$\begin{aligned} I = & I_{ph} - I_{o1} \left[\exp \left(\frac{V + IR_s}{V_{t1}} \right) - 1 \right] - I_{o2} \left[\exp \left(\frac{V + IR_s}{V_{t2}} \right) - 1 \right] \\ & - I_{o3} \left[\exp \left(\frac{V + IR_s}{V_{t3}} \right) - 1 \right] \frac{V + IR_s}{R_p} \end{aligned} \quad (5)$$

Note that the nine parameters are sensitive to operational conditions (solar irradiance and cell temperature). However, the PV arrays that consist of N_s modules are coupled in series to upturn the output voltage, and N_p modules are connected in parallel to increase the output current. Therefore, the output current of the PV arrays can be computed as:

$$\begin{aligned} I = & N_p I_{ph} - N_p I_{o1} \left[\exp \left(\frac{1}{V_{t1}} \left(\frac{V}{N_s} + \frac{IR_s}{N_p} \right) \right) - 1 \right] \\ & - N_p I_{o2} \left[\exp \left(\frac{1}{V_{t2}} \left(\frac{V}{N_s} + \frac{IR_s}{N_p} \right) \right) - 1 \right] \\ & - N_p I_{o3} \left[\exp \left(\frac{1}{V_{t3}} \left(\frac{V}{N_s} + \frac{IR_s}{N_p} \right) \right) - 1 \right] - \frac{N_p}{R_p} \left(\frac{V}{N_s} + \frac{IR_s}{N_p} \right) \end{aligned} \quad (6)$$

Thus, there are nine parameters (I_{ph} , I_{o1} , I_{o2} , I_{o3} , R_s , R_p , d_1 , d_2 and d_3) that required to be extracted to establish I–V and P–V curves [11].

2.2. Objective function

The objective of model construction and parameter extraction is to reduce the error between the computed and experimental currents at various environmental conditions. Thus, the nine parameters' estimation can be formulated using RMSE as an objective function that needs to be minimized.

It is essential to mention that Eq. (5) is a nonlinearity implicit transcendental equation and has nine unknown parameters. Several studies proposed methods to optimally extract these parameters, such as LM [69], NR [70–72], Taylor series (TS) [54], and Lambert W function [69]. According to the literature, two methods were often used for estimating the parameters of the PV models, which are the Newton Raphson method and the Lambert W function method as follows:

2.2.1. Newton Raphson method

In order to estimate the nine parameters of the PV models under particular weather conditions, the NR method is used for solving I–V curve equations, which can be given by the following [9,70,73]:

2.2.2. Lambert W function method

The lambert W function is used to mitigate the implicit coupling relation between the voltage and current. Therefore, the Lambert W function is employed to optimally extract the TD PV models' parameters due to its high precision, especially at a heterogeneous operating temperature [23,25,58,59]. The output current of the TD PV model based on the Lambert W function can therefore be represented as:

$$\begin{aligned} I = & \frac{R_p(I_{ph} + I_{o1} + I_{o2} + I_{o3}) - V}{R_p + R_s} - \frac{V_t}{R_s} [d_1 W(\beta_1) + d_2 W(\beta_2) \\ & + d_3 W(\beta_3)] \end{aligned} \quad (8)$$

where

$$\beta_1 = \frac{I_{o1} R_s R_p}{d_1 V_{t1} (R_s + R_p)} \exp \left\{ \frac{R_p (R_s I_{ph} + R_s I_{o1} + V)}{d_1 V_{t1} (R_s + R_p)} \right\} \quad (9)$$

$$\beta_2 = \frac{I_{o2} R_s R_p}{d_2 V_{t2} (R_s + R_p)} \exp \left\{ \frac{R_p (R_s I_{ph} + R_s I_{o2} + V)}{d_2 V_{t2} (R_s + R_p)} \right\} \quad (10)$$

$$\beta_3 = \frac{I_{o3} R_s R_p}{d_3 V_{t3} (R_s + R_p)} \exp \left\{ \frac{R_p (R_s I_{ph} + R_s I_{o3} + V)}{d_3 V_{t3} (R_s + R_p)} \right\} \quad (11)$$

2.2.3. The proposed improved NR (INR) meth

Even though the classical NR and lambert W function methods can deal with the nonlinearity of the PV model's equation, these approaches rapidly converge and rarely globally, leading to undesirable results, especially when the PV model's parameters that required to be extracted are large. In fact, the NR and lambert W function's performance at classical form may diverge from the real and exact root values. From a global perspective, it is essential to find global solutions in a few iterations and concisely. Thus, the proposed INR method can successfully increase the fraction of the steps to identify good initial conditions values [74,75]. The INR is given by,

$$I = I - \alpha \frac{dI}{dI'} \quad (12)$$

where

$$\begin{aligned} dI = & I_{ph} - I_{o1} \left(\exp \left(\frac{(V+IR_s)}{d_1 V_t} \right) - 1 \right) - I_{o2} \left(\exp \left(\frac{(V+IR_s)}{d_2 V_t} \right) - 1 \right) \\ & - I_{o3} \left(\exp \left(\frac{(V+IR_s)}{d_3 V_t} \right) - 1 \right) - \left(\left(\frac{V+IR_s}{R_p} \right) - I \right) \end{aligned} \quad (13)$$

$$I = I - \left(\frac{I_{ph} - I - I_{o1} \left(\exp \left(\frac{V+R_s I}{d_1 V_t} \right) - 1 \right) - I_{o2} \left(\exp \left(\frac{V+R_s I}{d_2 V_t} \right) - 1 \right) - I_{o3} \left(\exp \left(\frac{V+R_s I}{d_3 V_t} \right) - 1 \right) - \frac{V+R_s I}{R_p}}{-1 - I_{o1} \left(\frac{R_s}{d_1 V_t} \right) \exp \left(\frac{V+R_s I}{d_1 V_t} \right) - I_{o2} \left(\frac{R_s}{d_2 V_t} \right) \exp \left(\frac{V+R_s I}{d_2 V_t} \right) - I_{o3} \left(\frac{R_s}{d_3 V_t} \right) \exp \left(\frac{V+R_s I}{d_3 V_t} \right) - \frac{R_s}{R_p}} \right) \quad (7)$$

$$\begin{aligned} dI' = & - \left(I_{o1} \frac{R_s}{d_1 V_t} \left(\exp \left(\frac{(V+IR_s)}{d_1 V_t} \right) \right) \right) - \left(I_{o2} \frac{R_s}{d_2 V_t} \left(\exp \left(\frac{(V+IR_s)}{d_2 V_t} \right) \right) \right) \\ & - \left(I_{o3} \frac{R_s}{d_3 V_t} \left(\exp \left(\frac{(V+IR_s)}{d_3 V_t} \right) \right) \right) - \left(\frac{R_s}{R_p} \right) - 1 \end{aligned} \quad (14)$$

where α is chosen to be 0.05 after several attempts to reach the best stability rating. To meet the PV model's fluctuation nature at all the weather conditions, the epsilon value is assumed to be 0.03. For efficient and reliable estimation, the number of iterations is 3 for each data point value [76,77]. The MATLAB code of the INR method will be given in [Appendix 1](#). Please note that if the error between the pairs of the proposed and experimental currents are less than epsilon value, the program will stop and will take the second next pairs of data. This condition can significantly reduce the execution time at a very high of accuracy. The NR method has a curvature direction to reach the root of the I-V curve equation. Simultaneously, the lambert W function utilizes an exponential direction, and only INR can effectively predict the global solutions, as demonstrated in the results section. Thus, the objective function can be written as follows:

$$RMSE = \sqrt{1 / N \sum_{i=1}^N P(V_e, I_e, \theta)^2} \quad (15)$$

where N is the length of the I-V data curve, V_e and I_e are the experimental voltage and current of the PV model, while θ refers to the vector of the parameters required to be optimally extracted.

3. Enhanced LSHADE method

The DE method was firstly proposed by Storn and Price [78]. SHADE was ranked third in the IEEE CEC2013 competition, and the LSHADE was the winner of the CEC2014 competition [79,80]. It has been successfully implemented to solve real-world optimization problems [81,82]. In the basic DE algorithm, there are control parameters setting need to be adjusted [101], which are mutation factor (F), crossover rate (CR), and population size (P). The P consists of individual vectors (N_P) and each vector has a decision variable (D). Therefore, $i = 1, 2, \dots, N_P$ and $j = 1, 2, \dots, D$. The number of the maximum generation is (G_{max}) and used as a stopping criterion. Similar to the other stochastic population-based search methods, LSHADE method utilizes Mutation, External Archive, Parameter Adaption, Crossover, and Selection processes to find optimal values of the optimization problem. The main steps of the LSHADE method can be described as follows:

3.1. Initialization

The algorithm begins by randomly generating an initial population within feasible bounds of the decision variables. The initialization of the i -th component of the j -th decision variables can be written as following [6]:

$$X_{i,j}^{(0)} = X_{min,j} + Rand_{i,j} * (X_{max,j} - X_{min,j}) \quad (16)$$

where '0' represents the first initialization of the population, $Rand_{i,j}$ is randomly chosen within the range [0,1]. The next step is a mutation that produces a vector with each generation randomly.

3.2. Mutation

In each generation, a mutant vector $V_i^{(G)}$ is conducted from the population by applying 'current-to-pbest/1' and it can be expressed by the following [80]:

$$V_i^{(G)} = X_i^{(G)} + F_i^{(G)} (X_{pbest}^{(G)} - X_i^{(G)}) + F_i^{(G)} (X_{R_1^{(G)}}^{(G)} - X_{R_2^{(G)}}^{(G)}) \quad (17)$$

The $R_1^{(G)}$ and $R_2^{(G)}$ are two distinct vectors randomly selected from the N_P . $X_{pbest}^{(G)}$ is the first rank vector from the $N_P \times k$ ($k \in [0, 1]$), k is the control parameter and assumed to be small value for more greedily, and $F_i^{(G)}$ is the mutation scale parameters, and it is changeable with each generation.

3.3. External archive

LSHADE utilizes an external archive to increase the diversification of the parent vectors $X_i^{(G)}$. When the archive is utilized, the $X_i^{(G)}$ is chosen from the population and archive $P \cup A$. The size of the P and A is designed to be the same. Whenever the size of the archive is exceeds $|A|$, deletion is performed to insert the new elements.

3.4. Parameter adaption

The adaption of parameters mutation scale $F_i^{(G)}$ and crossover rate $CR_i^{(G)}$ is associated with each individual vector $X_i^{(G)}$ to generate the offspring vector $U_i^{(G)}$, where the adaption of these two parameters can be given by,

$$F_i^{(G)} = Rand_i(M_F, 0.1) \quad (18)$$

$$CR_i^{(G)} = Rand_i(M_{CR}, 0.1) \quad (19)$$

where $Rand_i(M_F, 0.1)$ and $Rand_i(M_{CR}, 0.1)$ are values sampled from the Cauchy and normal distributions. The range of the $F_i^{(G)}$ and $CR_i^{(G)}$ values are should be within the range [0, 1]. The $F_i^{(G)}$ is truncated if it is larger than 1, and it will be repeated by Eq. (18) until reaching a valid value if it is less than 0. Both M_F and M_{CR} are set to be 0.5 at the beginning of the search [81].

At generation G , if the offspring vector survives after competition with the parent vector, the current values of the $F_i^{(G)}$ and $CR_i^{(G)}$ values are assumed to be successful and stored in S_F and S_{CR} , respectively. The content of the memory of M_F and M_{CR} , at the end of the generation, is updated using weighted Lehmer mean and weighted arithmetic mean as follows [81]:

$$M_{F,k}^{(G)} = \begin{cases} mean_{WL}(S_F) & \text{if } (S_F) \neq \emptyset \\ M_{F,k}^{(G)}, & \text{otherwise} \end{cases} \quad (20)$$

$$M_{CR,k}^{(G)} = \begin{cases} mean_{WA}(S_{CR}) & \text{if } (S_{CR}) \neq \emptyset \\ M_{CR,k}^{(G)}, & \text{otherwise} \end{cases} \quad (21)$$

where k is an index with memory size (H) ($1 \leq k \leq H$) determines the memory's location to be updated. At first, the k value is set to 1, and then it is incremented if a new element is inserted into memory. k is set to be one if its value is larger than H . Note that the memory will not be updated if the individuals in generation G fail to generate an offspring vector.

3.5. Crossover

To generate the offspring vector $U_{i,j}^{(G)}$, the mutant vector $V_{i,j}^{(G)}$ mixes its components with the target (parent) vector $X_{i,j}^{(G)}$ and it uses a binomial scheme as follows:

$$U_{i,j}^{(G)} = \begin{cases} V_{i,j}^{(G)} & \text{if } j = j_{Rand} \text{ OR } Rand_{i,j}[0, 1] \leq CR_i^{(G)} \\ X_{i,j}^{(G)}, & \text{otherwise} \end{cases} \quad (22)$$

where j_{Rand} is randomly chosen within the range of $[1, D]$ and $CR_i^{(G)}$ is a value in the range $[0, 1]$.

3.6. Selection

In this process, a comparison is performed between the parents and offering vectors; the fittest vector is chosen for the next generation.

$$X_i^{(G)} = \begin{cases} U_{i,j}^{(G)} & \text{if } f(U_{i,j}^{(G)}) \leq f(X_i^{(G)}) \\ X_i^{(G)}, & \text{otherwise} \end{cases} \quad (23)$$

3.7. Linear population size reduction (LPSR)

The performance of the LSHADE is improved by using linear population size reduction for each generation, where the size of the population is dynamically reduced as follows [79]:

$$N_p = \text{round} \left[\left(\frac{N_{p,\min} - N_{p,\text{ini}}}{G_{\max}} \right) * NFE + N_{p,\text{ini}} \right] \quad (24)$$

where $N_{p,\min}$ is the minimum number of the population, here the $N_{p,\min}$ is assumed to be 4, $N_{p,\text{ini}}$ is the initial value of the population size, NFE is the number of fitness function evaluations, and G_{\max} is the maximum number of the fitness function evaluations.

3.8. The proposed enhanced LSHADE method

To enrich the population diversity and boost the convergence ability of the LSHADE algorithm, we divided the size of the population into two parts. In the first part, the current-to-pbest/ 1' scheme is used as it in Eq. (17). Contrarily, the second section of the

population performs the guided-chaotic strategy as follows [8]:

$$V_i^{(G)} = X_{i,j}^{(G)} + Rand_1 \cdot (X_{\text{best},j}^{(G)} - X_{i,j}^{(G)}) - O \cdot Rand_2 \cdot (X_{\text{worst},j}^{(G)} - X_{i,j}^{(G)}) \quad (25)$$

where O is a chaotic perturbation, and it is given by,

$$x_{NFE+1} = 4 \cdot x_{NFE} \cdot (1 - x_{NFE})$$

where

$$O = x_{NFE+1} \quad (26)$$

Chaos has the benefit of the pseudo-random patterns within the cycles [83,112–114]. The chaotic distribution is used to explore new search areas, which leads to enhance searching direction from locality to globally, as demonstrated in Fig. 2.

Therefore, the cooperative hybrid strategy has several advantages: first, it benefits from the high-exploitation ability in the first part of the population size. Second, the exploration tendency is strengthened to search for new promising areas by using a chaotic distribution mechanism that can substantially escape falling into the locality. Simultaneously, the quality of the solutions is enhanced rather than wait for the next generation. In comparison, dividing the search space into sub-region can balance the exploration and exploitation phases and convergence very fast at a small number of generations. Finally, reliable and successful results can be achieved at every execution, which can guarantee global solutions. The operation process of the ELSHADE method is illustrated in Fig. 3.

4. Results and discussions

To verify the accuracy, stability, reliability, and convergence of the proposed ELSHADE-INR method, a real experimental data of (Kyocera KC120-1 multi-crystalline) PV module under arbitrary conditions and compared with well-regard published papers based on several evaluation criteria analysis [25]. Under Standard Test Conditions (STC), this PV module's specification is given in Table 1, and the number of the I–V curve data points is tabulated in Table 2. While the evaluation criteria are Root Mean Square Error (RMSE), Mean Bias Error (MBE), Determination Coefficient (R^2), RMSE deviation for each level of solar radiation (d_i), Standard Test Deviation (STD), Absolute Error (AE), and Test Statistical (TS). The methods used for comparison are ELSHADE-LW, ELSHADE, PGJAYA [8], CLPSO [84], MLBSA [50], MRFQ [68], MPALW [67], and LCROA [66].

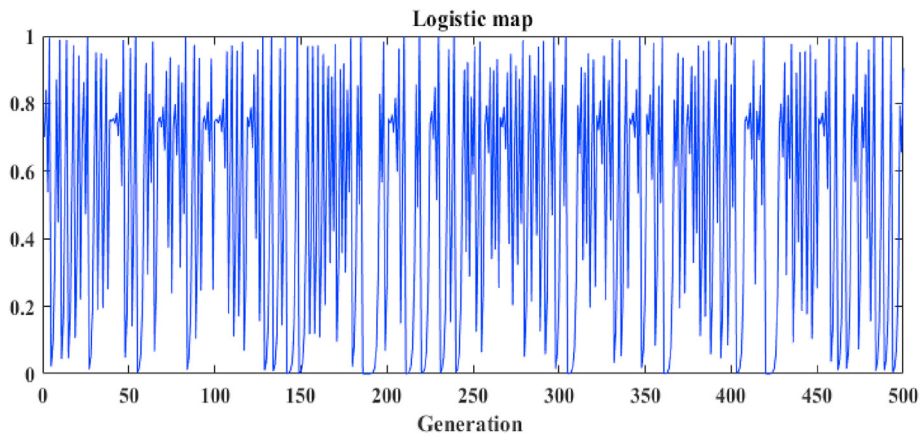
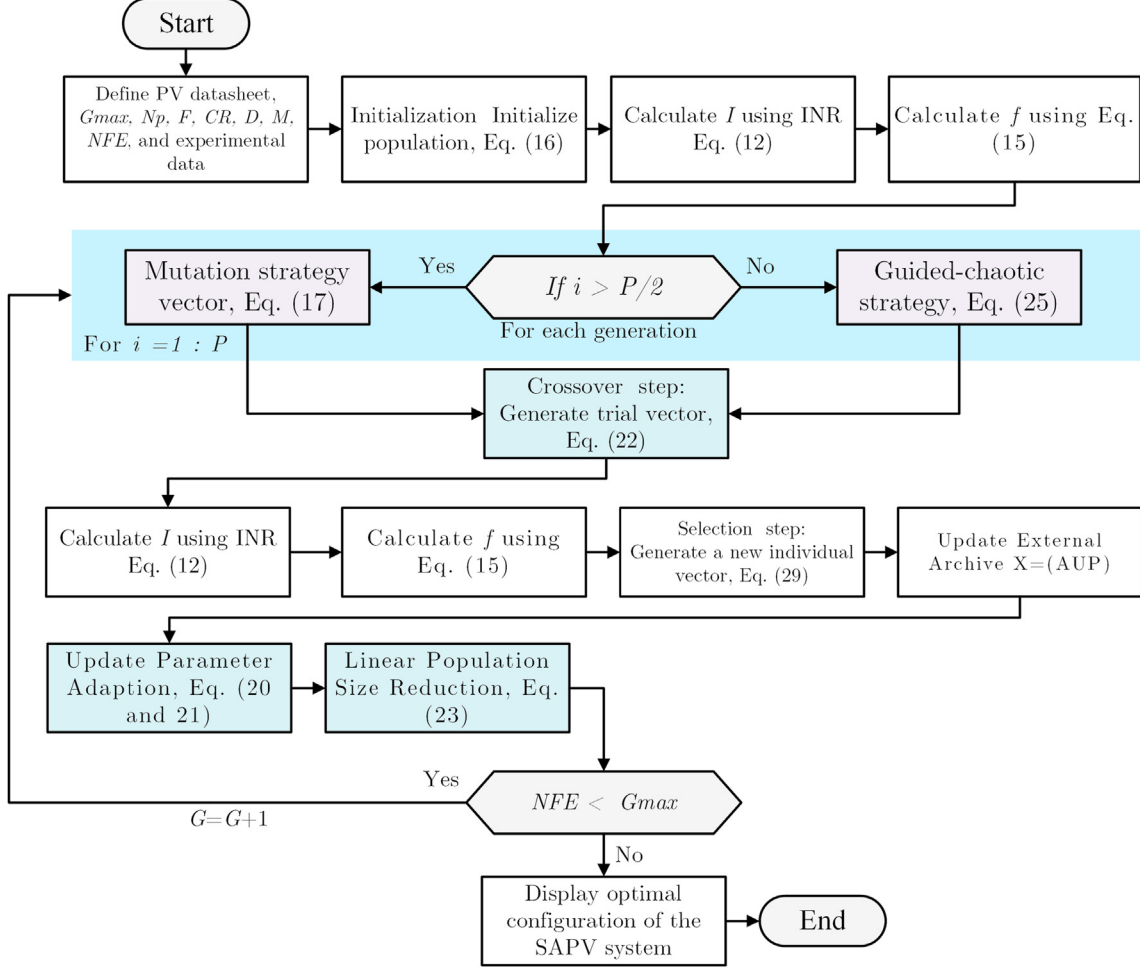


Fig. 2. Visualization of the chaotic map.

**Fig. 3.** Flowchart of the proposed ELSHADE-INR method.**Table 1**
Specifications of the (Kyocera KC120-1) PV module.

Characteristics	Value
Maximum power at STC	120 (Wp)
Current at MPP (I_{mp})	7.1 (A)
The voltage at MPP (V_{mp})	16.9 (V)
Short-circuit current (I_{sc})	7.45 (A)
Open-circuit voltage (V_{oc})	16.9 (V)
Nominal Operation Cell Temperature (NOCT)	43.6 (°C)
Temperature coefficient of I_{sc} (α)	1.325 (mA/k)
Temperature coefficient of V_{sc} (β)	-77 (mV/k)

Table 2
Data points of the real experimental data under nonstandard test conditions.

Weather condition	S_1	S_2	S_3	S_4	S_5	S_6	S_7
Data points' length	22	24	50	91	92	101	102

It is worth mentioning that the objective function of ELSHADE-LW is based on the Lambert W function, while the ELSHADE-INR and ELSHADE are based on improved NR and original NR methods, respectively.

The ELSHADE-INR method is used for parameter extraction of the TD PV module's model. For a fair comparison, all the setting environmental are set the same. This is to understand that there is

no bias because of systems, or pre-conditions, as per artificial intelligence literature. The number of generation (G_{max}) is 500, the size of the population (P) is 50, memory size (H) is 5, the dimension of the problem (D) is 9, and the archive rate is 1.4, where each algorithm should run 30 individually. The search space of the nine parameters ($d_1, d_2, d_3, I_{ph}, I_{o1}, I_{o2}, I_{o3}, R_s, R_p$) are [1,2] for d_1 and d_2 , [0.5, 8] for I_{ph} , [$1e^{-12}, 1e^{-5}$] for I_{o1}, I_{o2} , and I_{o3} , [0.1, 2] for R_s , and [10, 8000] for R_p [9,85]. In general, the ideality factors for all types of PV modules are assumed to be within a range of $1 < d_1, d_2 < 2$ for SD, DD, and TD PV models. In meanwhile, the third ideality factor of the TD PV model for C-Si PV module increases by increasing defect density and can reach to 5. The d_3 belongs to the range [1,5] as mentioned on Ref. [86]. This is due to increasing in Donor-Acceptor Pairs, which is proportional to increasing the recombination rate [86]. It is worth mentioning that the diode's ideality factor decreases over time because of joule heating's effects [87]. Note that the overall best statistical values are marked in **boldface** in all Tables. **boldface** in all Tables.

The extracted nine parameters of the TD solar module for all involved methods are listed in Table 3. It can obviously note that the I_{ph} value increased linearly with solar irradiance increasing, which reflects the physical perspective. While the d_{1-2} and I_{o1-3} are almost kept within ranges (1.0004–1.9842) and (1.84E-06 and 3.49E-12), except for the d_3 are changeable up to 5. The reasons for that are because of the increasing defect density for the diode ideality factor and enhancement of photon absorption due to the

Table 3

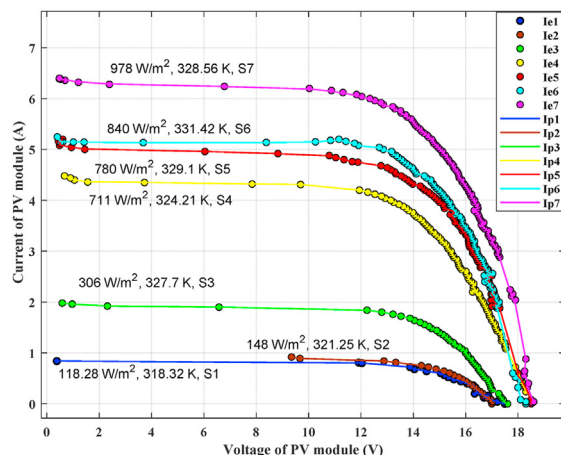
Results of the predicted parameters of the TD PV module by various algorithms.

Parameter	Method	S_1	S_2	S_3	S_4	S_5	S_6	S_7
d_1	ELSHADE-INR	1.0839	1.9727	1.0004	1.2042	1.5389	1.3856	1.3934
	ELSHADE-LW	1.0363	1.3896	1.9999	1.2051	1.9304	1.5025	1.6516
	ELSHADE	1.0000	1.5283	2.0000	1.1501	1.8032	1.4840	1.4984
	PGJAYA	2.0000	1.4137	1.1661	1.2604	2.0000	1.4538	1.4677
	CPSO	1.0000	1.7858	1.1547	1.3254	1.7134	1.4533	1.5030
	MLBSA	1.9999	1.9329	1.5502	1.9563	1.2929	1.4266	1.4996
	MRFO	1.9786	1.4182	2.0000	1.9627	1.5306	1.4096	1.4540
	MPALW	1.0000	1.1720	1.9999	1.9975	1.3313	1.4880	1.6403
d_2	LCROA	1.9922	1.6016	1.7273	1.9892	1.3102	1.4627	1.7030
	ELSHADE-INR	1.9842	1.2460	1.0846	1.1322	1.2288	1.4842	1.5789
	ELSHADE-LW	1.9968	1.9843	1.0886	1.9999	1.1548	1.5763	1.6500
	ELSHADE	1.0000	1.2165	1.0913	1.1762	1.4140	1.4490	1.4993
	PGJAYA	1.0000	1.9803	1.9181	1.8995	1.5761	1.4505	1.4849
	CPSO	1.4541	1.3276	1.6373	1.3902	1.2048	1.4317	1.4996
	MLBSA	1.0067	1.2746	1.0603	1.5792	1.9999	1.4708	1.4988
	MRFO	1.0805	1.7936	1.1910	1.3419	1.2575	1.5500	1.6873
d_3	MPALW	2.0000	1.8929	1.1349	1.2514	1.8724	1.4870	1.5392
	LCROA	1.0174	1.3015	1.1716	1.2871	1.6783	1.4297	1.3800
	ELSHADE-INR	4.8592	1.1944	4.9996	4.9513	4.9998	4.6709	4.9100
	ELSHADE-LW	4.9959	1.8118	2.5681	2.9385	2.3733	1.3777	1.5545
	ELSHADE	5.0000	5.0000	1.0000	4.7204	1.0000	1.4826	1.4992
	PGJAYA	1.8091	3.5696	2.4415	2.6379	1.3121	1.4594	1.5546
	CPSO	4.7101	3.9629	4.9464	4.4267	2.0537	1.5090	1.4944
	MLBSA	1.0000	4.9772	1.4375	1.2046	5.0000	1.5440	1.4985
I_{ph}	MRFO	4.9026	5.0000	2.3894	4.0568	4.9291	1.4392	1.4680
	MPALW	4.7872	4.9698	3.7748	4.9999	4.9997	2.6581	1.6502
	LCROA	2.9725	1.8999	2.0120	2.0492	3.3814	1.5017	3.9124
	ELSHADE-INR	0.8416	1.0023	1.9713	4.4469	5.1618	5.1513	6.4873
	ELSHADE-LW	0.8380	0.9476	1.9598	4.4416	5.1778	5.2001	6.4612
	ELSHADE	0.8402	0.9938	1.9608	4.4474	5.1622	5.1853	6.4479
	PGJAYA	0.8430	0.9240	1.9584	4.4189	5.1398	5.1784	6.4640
	CPSO	0.8401	0.9606	1.9557	4.4181	5.1461	5.1806	6.4455
I_{o1}	MLBSA	0.8402	0.9702	1.9604	4.4437	5.1520	5.1838	6.4464
	MRFO	0.8350	0.9403	1.9481	4.4150	5.1547	5.1701	6.4508
	MPALW	0.8406	0.9828	1.9588	4.4357	5.1390	5.1906	6.4540
	LCROA	0.8284	0.9119	1.9428	4.3968	5.0744	5.1885	6.3382
	ELSHADE-INR	7.67E-08	6.19E-08	6.21E-08	5.89E-07	1.34E-06	9.99E-06	9.99E-06
	ELSHADE-LW	3.61E-08	3.94E-06	1.00E-12	9.82E-07	9.99E-06	8.69E-06	1.00E-05
	ELSHADE	2.16E-11	1.00E-12	4.97E-10	5.32E-09	1.00E-05	9.99E-06	1.00E-05
	PGJAYA	1.00E-12	4.72E-06	7.27E-07	1.96E-06	4.74E-06	9.99E-06	1.00E-05
I_{o2}	CPSO	1.94E-08	2.46E-08	6.36E-07	4.06E-06	9.79E-06	7.60E-06	9.99E-06
	MLBSA	5.00E-12	1.88E-06	1.00E-12	8.57E-10	3.94E-06	9.87E-06	9.99E-06
	MRFO	3.14E-07	4.88E-06	1.00E-05	4.36E-09	1.40E-07	9.97E-06	9.96E-06
	MPALW	1.94E-08	3.31E-07	1.00E-12	9.41E-08	6.01E-06	9.99E-06	7.97E-06
	LCROA	2.67E-06	2.77E-06	4.44E-06	1.42E-06	4.46E-06	9.88E-06	3.74E-06
	ELSHADE-INR	1.69E-10	4.25E-07	3.49E-12	1.46E-07	1.84E-06	9.90E-06	9.31E-06
	ELSHADE-LW	1.00E-12	3.14E-09	2.49E-07	6.22E-07	6.41E-07	1.00E-05	9.99E-06
	ELSHADE	1.94E-08	6.55E-07	2.64E-07	6.70E-07	5.50E-06	1.00E-05	1.00E-05
I_{o3}	PGJAYA	1.95E-08	8.24E-06	2.65E-06	1.87E-07	1.00E-12	1.00E-05	1.00E-05
	CPSO	3.67E-11	2.18E-06	1.03E-09	1.94E-08	1.30E-06	9.98E-06	9.99E-06
	MLBSA	1.00E-12	1.24E-06	1.65E-07	9.18E-10	8.45E-06	1.00E-05	9.99E-06
	MRFO	7.14E-08	2.73E-06	9.83E-07	4.85E-06	2.67E-06	2.11E-08	9.68E-06
	MPALW	1.28E-08	9.27E-06	4.88E-07	1.76E-06	1.21E-12	9.98E-06	9.99E-06
	LCROA	2.50E-08	1.37E-06	7.62E-07	2.64E-06	8.14E-06	9.37E-06	1.00E-05
	ELSHADE-INR	9.98E-06	2.67E-07	9.66E-06	9.85E-06	3.94E-08	3.33E-06	4.80E-09
	ELSHADE-LW	1.29E-07	1.00E-12	1.00E-05	1.04E-12	9.99E-06	7.12E-07	1.00E-05
R_s	ELSHADE	1.00E-05	2.81E-07	1.00E-12	1.00E-12	3.55E-08	9.99E-06	9.99E-06
	PGJAYA	6.30E-07	1.00E-05	8.84E-06	1.00E-05	4.89E-06	6.02E-06	9.24E-06
	CPSO	4.06E-09	4.79E-06	1.97E-06	7.34E-06	6.37E-06	9.95E-06	9.99E-06
	MLBSA	1.94E-08	1.00E-05	1.00E-12	9.87E-07	7.41E-11	9.99E-06	9.99E-06
	MRFO	1.17E-06	1.00E-12	1.00E-12	1.00E-12	8.67E-07	9.98E-06	9.28E-06
	MPALW	1.89E-06	3.37E-06	8.47E-06	9.99E-06	1.40E-07	9.99E-06	9.71E-06
	LCROA	8.97E-06	8.69E-06	1.34E-06	4.41E-06	8.42E-06	8.26E-06	5.92E-06
	ELSHADE-INR	1.7782	0.3955	0.7759	0.5645	0.2928	0.1641	0.1531
R_p	ELSHADE-LW	1.8915	0.2325	0.7280	0.5573	0.3406	0.4138	0.3680
	ELSHADE	1.9322	0.4164	0.7244	0.5640	0.3107	0.1647	0.1557
	PGJAYA	1.9934	0.2097	0.6793	0.5390	0.2710	0.1688	0.1484
	CPSO	1.9325	0.0395	0.6751	0.5138	0.1679	0.1679	0.1560
	MLBSA	1.9323	0.3564	0.7383	0.5533	0.2750	0.1671	0.1561
	MRFO	1.8380	0.1814	0.6570	0.5089	0.2867	0.1783	0.1621
	MPALW	1.9318	0.5094	0.6920	0.5380	0.2689	0.3187	0.3667
	LCROA	1.9425	0.3209	0.6864	0.5327	0.2899	0.1636	0.1853
R_p	ELSHADE-INR	911.35	103.12	141.79	103.09	38.95	2932.19	27.92
	ELSHADE-LW	1866.96	239.76	211.75	116.38	36.32	7973.14	42.95

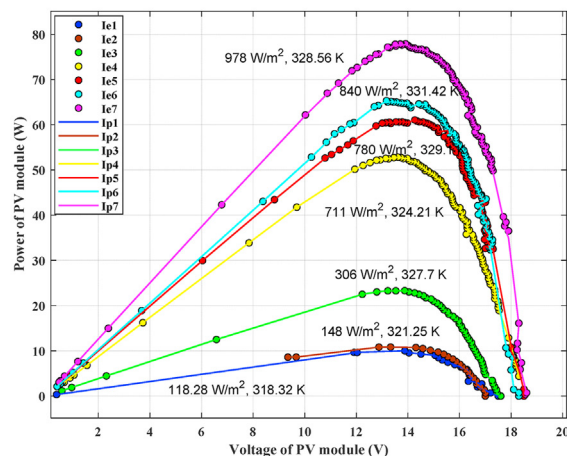
Table 3 (continued)

Parameter	Method	S_1	S_2	S_3	S_4	S_5	S_6	S_7
ELSHADE		1131.52	112.08	217.73	102.12	40.02	7993.47	35.06
PGJAYA		8000.00	552.41	331.41	194.15	44.93	7976.44	32.00
CPSO		1125.04	181.56	275.97	235.31	39.93	6618.00	35.39
MLBSA		1118.18	152.24	186.95	111.61	42.47	6802.45	35.30
MRFO		8000.00	297.64	542.13	287.85	40.32	6960.59	34.26
MPALW		1072.51	131.02	247.40	137.59	46.19	7999.96	43.82
LCROA		7195.28	1161.55	5143.18	427.56	86.37	6170.47	42.55

(a)



(b)

**Fig. 4.** Comparison between the proposed and experimental data of the ELSHADE-INR method for the TD PV module at seven weather conditions (a) I–V curve (b) P–V curve.

variation of the ambient temperature, where the I_{01-3} values are positively correlated with the temperature. Bearing in mind, the INR method has a very high sensitivity to the ideality factor values, which means that selecting an appropriate ideality factor value leads to the divergence of the ELSHADE-INR method during the optimization process. Finally, the R_p and R_s values are dramatically decreased from approximately 911.35 and 1.77 to 27.92 and 0.153, respectively. According to Table 3, the ELSHADE-INR has the best dispersion of the TD PV model parameters. This can confirm that the proposed ELSHADE based on the INR method can accurately find the parameters' root values and provide a very high level of

stability during the running of the algorithm. Therefore, the predicted I–V and PV curves for the TD PV model using the ELSHADE-INR method is illustrated in Fig. 4. It can be clearly noted that the proposed model has very high coincidence with the experimental data under all-weather conditions. This means that the ELSHADE-INR can actually predict the experimental currents for the TD PV model at different arbitrary conditions.

For more convenience, various comparative analyses are carried out to illustrate the surpassing of the ELSHADE-INR methods against other peers. The accuracy can be measured by minimizing RMSE, MBE, and TS values, while the reliability can be determined by minimum AE and STD values. In comparison, the consistent performance of the R^2 value is expected to be higher and close to 1. The outcomes of the ELSHADE-INR and other methods for the TD PV model based on several statistical criteria are tabulated in Table 4.

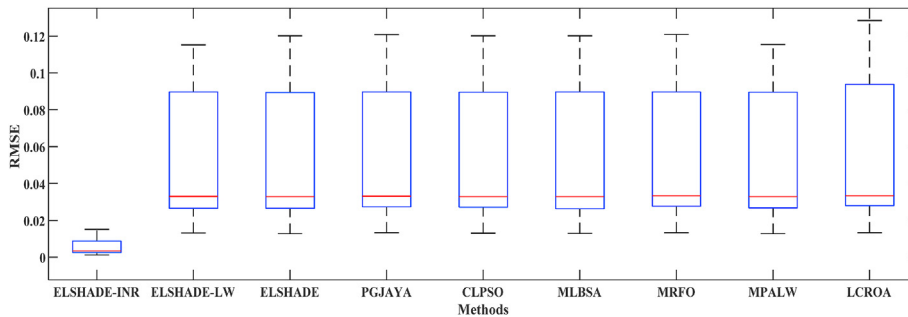
Table 4 indicates that the ELSHADE-INR outperformed all eight methods in terms of accuracy, stability, and it can be found to be more robust compared with other methods. In terms of accuracy, the ELSHADE-INR has minimum RMSE values under all weather conditions, where the average RMSE value is 0.0060, followed by ELSHADE-LW with 0.0560 in the second rank. MPALW is located in the third rank, while ELSHADE and MLBSA share the 4th rank with 0.0566. Then, LCROA and MRFO came with the worst average RMSE values, 0.0592 and 0.0573, followed by PGJAYA and CPSO with 0.0571 and 0.0569, respectively. Nevertheless, the ELSHADE/LW, MPALW, and MLBSA methods can reach the specific RMSE value at each execution, but their average RMSE values are larger than ELSHADE-INR. This is because ELSHADE-INR can effectively discover search space and return precise nine parameter values during the TD PV module's optimization. ELSHADE-INR can practically deal with the TD PV module's transcendent equation, which can not be solved linearly. As a result, the TD PV model's global solutions can be sufficiently extracted by this method. Similarly, the ELSHADE-INR dominates other methods in terms of MBE, R^2 , d_i , STD, and TS statistical analysis, where their average values are 5.88×10^{-5} , 0.9999, 2.54E-05, 0.0050, and 0.0538, respectively. The 2nd rank can be taken by ELSHADE-LW, followed by MPALW, ELSHADE, MLBSA, CLPSO, PGJAYA, MRFO, and LCROA, as demonstrated in Table 4.

For further visual verification superiority performance of the proposed ELSHADE-INR model, all models' boxplot is presented in Fig. 5. It can be seen that the ELSHADE-INR has the minimum RMSE values. Simultaneously, the PGJAYA, MRFO, and LCROA show unstable efficacy and could be stuck in local optima, mainly when the optimization problem is multidimensional and has noise effects. Moreover, Figs. 6 and 7 exhibits the statistical criteria of the MBE, R^2 , and TS for all models based on real experimental data. It can be perceived that the ELSHADE-INR is always able to outperform other models. This is because it is a high capability in obtaining delicate exploitation and exploration tendencies in the proposed algorithm itself and in the improved formulation of the objective function meaningfully. It is worth mentioning that the real experimental data has noise characteristics, and the TD PV module is multi-

Table 4

Statistical results of various methods for the TD PV model.

Parameter	Method	S_1	S_2	S_3	S_4	S_5	S_6	S_7	Average
RMSE	ELSHADE-INR	0.0034	0.0012	0.0024	0.0027	0.0087	0.0088	0.0151	0.0060
	ELSHADE-LW	0.0330	0.0131	0.0260	0.0280	0.0909	0.0858	0.1153	0.0560
	ELSHADE	0.0329	0.0127	0.0260	0.0280	0.0904	0.0861	0.1201	0.0566
	PGJAYA	0.0331	0.0133	0.0269	0.0284	0.0909	0.0863	0.1208	0.0571
	CPSO	0.0329	0.0130	0.0265	0.0288	0.0906	0.0863	0.1201	0.0569
	MLBSA	0.0329	0.0129	0.0257	0.0280	0.0908	0.0862	0.1201	0.0566
	MRFO	0.0333	0.0133	0.0272	0.0290	0.0907	0.0868	0.1209	0.0573
	MPALW	0.0329	0.0127	0.0263	0.0282	0.0909	0.0860	0.1154	0.0561
MBE	LCROA	0.0333	0.0133	0.0277	0.0290	0.0961	0.0867	0.1284	0.0592
	ELSHADE-INR	1.16E-05	1.55E-06	5.89E-06	7.43E-06	7.60E-05	7.86E-05	2.30E-04	5.88E-05
	ELSHADE-LW	1.09E-03	1.74E-04	6.78E-04	7.86E-04	8.28E-03	7.38E-03	1.33E-02	4.53E-03
	ELSHADE	1.08E-03	1.63E-04	6.77E-04	7.84E-04	8.19E-03	7.43E-03	1.44E-02	4.68E-03
	PGJAYA	1.10E-03	1.78E-04	7.25E-04	8.08E-04	8.27E-03	7.46E-03	1.46E-02	4.73E-03
	CPSO	1.08E-03	1.70E-04	7.07E-04	8.33E-04	8.22E-03	7.45E-03	1.44E-02	4.70E-03
	MLBSA	1.08E-03	1.67E-04	6.63E-04	7.86E-04	8.25E-03	7.44E-03	1.44E-02	4.69E-03
	MRFO	1.11E-03	1.77E-04	7.41E-04	8.43E-04	8.23E-03	7.54E-03	1.46E-02	4.75E-03
R^2	MPALW	1.08E-03	1.63E-04	6.97E-04	7.97E-04	8.28E-03	7.40E-03	1.33E-02	4.54E-03
	LCROA	1.11E-03	1.78E-04	7.68E-04	8.47E-04	9.25E-03	7.53E-03	1.65E-02	5.17E-03
	ELSHADE-INR	0.9998	0.9999						
	ELSHADE-LW	0.9834	0.9977	0.9980	0.9993	0.9949	0.9958	0.9943	0.9948
	ELSHADE	0.9835	0.9978	0.9980	0.9993	0.9949	0.9957	0.9938	0.9947
	PGJAYA	0.9833	0.9976	0.9978	0.9993	0.9949	0.9957	0.9937	0.9946
	CPSO	0.9835	0.9977	0.9979	0.9993	0.9949	0.9957	0.9938	0.9947
	MLBSA	0.9836	0.9978	0.9980	0.9993	0.9949	0.9957	0.9938	0.9947
d_i	MRFO	0.9823	0.9977	0.9978	0.9993	0.9949	0.9957	0.9937	0.9946
	MPALW	0.9835	0.9978	0.9979	0.9993	0.9949	0.9958	0.9942	0.9948
	LCROA	0.9831	0.9976	0.9977	0.9993	0.9943	0.9957	0.9929	0.9944
	ELSHADE-INR	-0.0026	-0.0048	-0.0036	-0.0033	0.0026	0.0027	0.0091	2.5E-05
	ELSHADE-LW	-0.0230	-0.0428	-0.0300	-0.0280	0.0349	0.0298	0.0592	0.0016
	ELSHADE	-0.0237	-0.0438	-0.0306	-0.0286	0.0338	0.0295	0.0635	0.0017
	PGJAYA	-0.0239	-0.0438	-0.0302	-0.0287	0.0337	0.0292	0.0637	0.0017
	CPSO	-0.0240	-0.0439	-0.0303	-0.0280	0.0337	0.0293	0.0632	0.0017
TS	MLBSA	-0.0240	-0.0440	-0.0312	-0.0289	0.0338	0.0293	0.0634	0.0017
	MRFO	-0.0240	-0.0440	-0.0301	-0.0283	0.0333	0.0294	0.0636	0.0017
	MPALW	-0.0231	-0.0433	-0.0297	-0.0278	0.0348	0.0299	0.0593	0.0016
	LCROA	-0.0259	-0.0459	-0.0315	-0.0301	0.0368	0.0274	0.0691	0.0019
	ELSHADE-INR	0.0156	0.0059	0.0048	0.0258	0.0831	0.0887	0.1527	0.0538
	ELSHADE-LW	0.1514	0.0632	0.0520	0.2660	0.8716	0.8620	1.1667	0.4904
	ELSHADE	0.1509	0.0611	0.0520	0.2657	0.8668	0.8650	1.2163	0.4968
	PGJAYA	0.1521	0.0639	0.0538	0.2698	0.8708	0.8669	1.2234	0.5000
	CPSO	0.1509	0.0624	0.0532	0.2738	0.8683	0.8664	1.2163	0.4988
	MLBSA	0.1509	0.0619	0.0514	0.2661	0.8698	0.8657	1.2163	0.4975
	MRFO	0.1527	0.0637	0.0544	0.2775	0.8692	0.8715	1.2249	0.5017
	MPALW	0.1509	0.0611	0.0528	0.2680	0.8716	0.8635	1.1685	0.4909
	LCROA	0.1530	0.0640	0.0554	0.2761	0.9217	0.8709	1.3019	0.5204

**Fig. 5.** Boxplot of the average RMSE values for the ELSHADE-INR and other models under seven weather conditions.

model optimization. Thus, any reduction in RMSE values is significant and reflects the proposed ELSHADE-INR model's high accuracy.

To further assess the efficiency of the proposed ELSHADE-INR method relative to other peers, the average and individual AEs values are computed at each level of the solar radiation and ambient temperature by maintaining actual experimental data as

in [Table 5](#) and [Fig. 8](#), respectively. To be specific, it can be noted that the ELSHADE-INR has deficient absolute error compared with other methods, which reflects the good coincided with the measured currents. However, the AE may increase at high levels of solar radiation. It is worth mentioning that the key to the improvement in the objective function can offer global parameter extraction of the TD PV model, which confirms the excellent stability and reliability

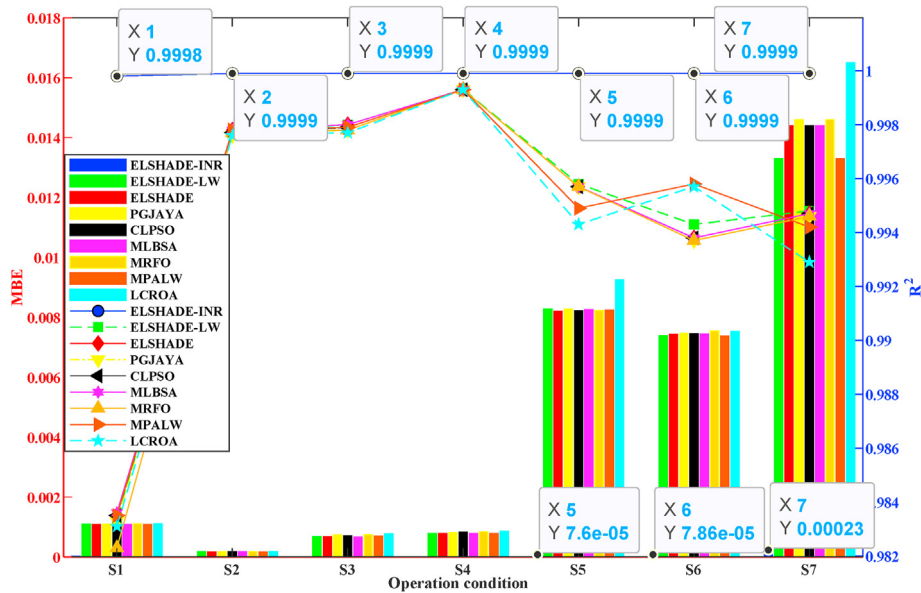
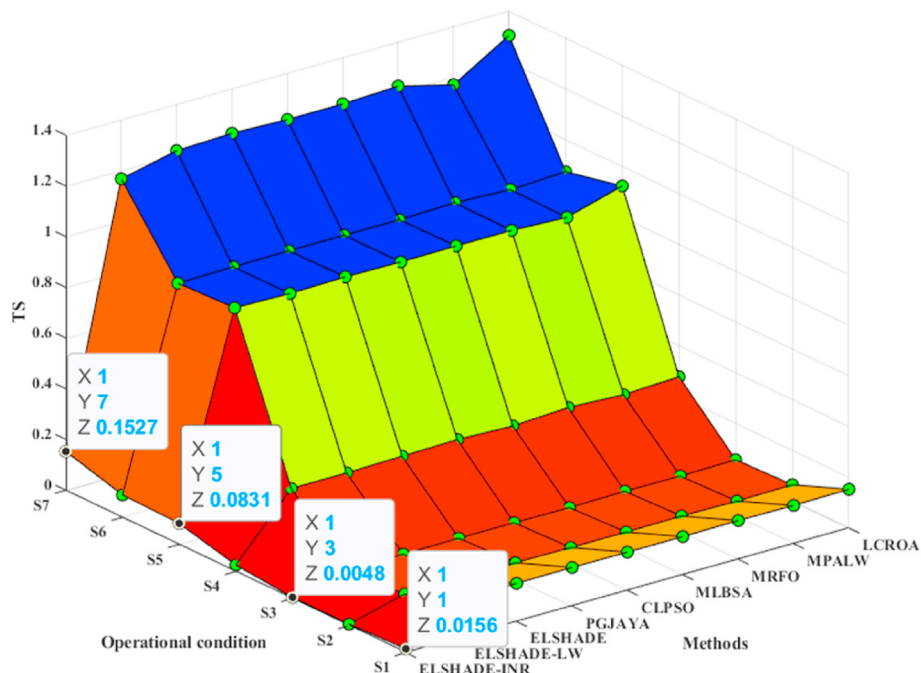
Fig. 6. MBE and R^2 values for the ELSHADE-INR and other algorithms under real experimental data.

Fig. 7. Comparison between ELSHADE-INR and other methods at various operational conditions for the TD PV model.

Table 5

Average AE of various methods under seven weather conditions.

Method	S_1	S_2	S_3	S_4	S_5	S_6	S_7	Avg.
ELSHADE-INR	0.0023	0.0008	0.0016	0.0019	0.0059	0.0066	0.0102	0.0042
ELSHADE-LW	0.0238	0.0102	0.0180	0.0218	0.0632	0.0800	0.0846	0.0431
ELSHADE	0.0235	0.0096	0.0182	0.0218	0.0625	0.0825	0.0903	0.0441
PGJAYA	0.0243	0.0103	0.0193	0.0216	0.0619	0.0835	0.0919	0.0447
CLPSO	0.0235	0.0100	0.0188	0.0221	0.0621	0.0832	0.0903	0.0443
MLBSA	0.0235	0.0099	0.0178	0.0218	0.0618	0.0827	0.0903	0.0440
MRFO	0.0242	0.0104	0.0196	0.0221	0.0623	0.0849	0.0909	0.0449
MPALW	0.0235	0.0096	0.0186	0.0219	0.0618	0.0816	0.0847	0.0431
LCROA	0.0242	0.0103	0.0206	0.0220	0.0698	0.0839	0.1022	0.0476

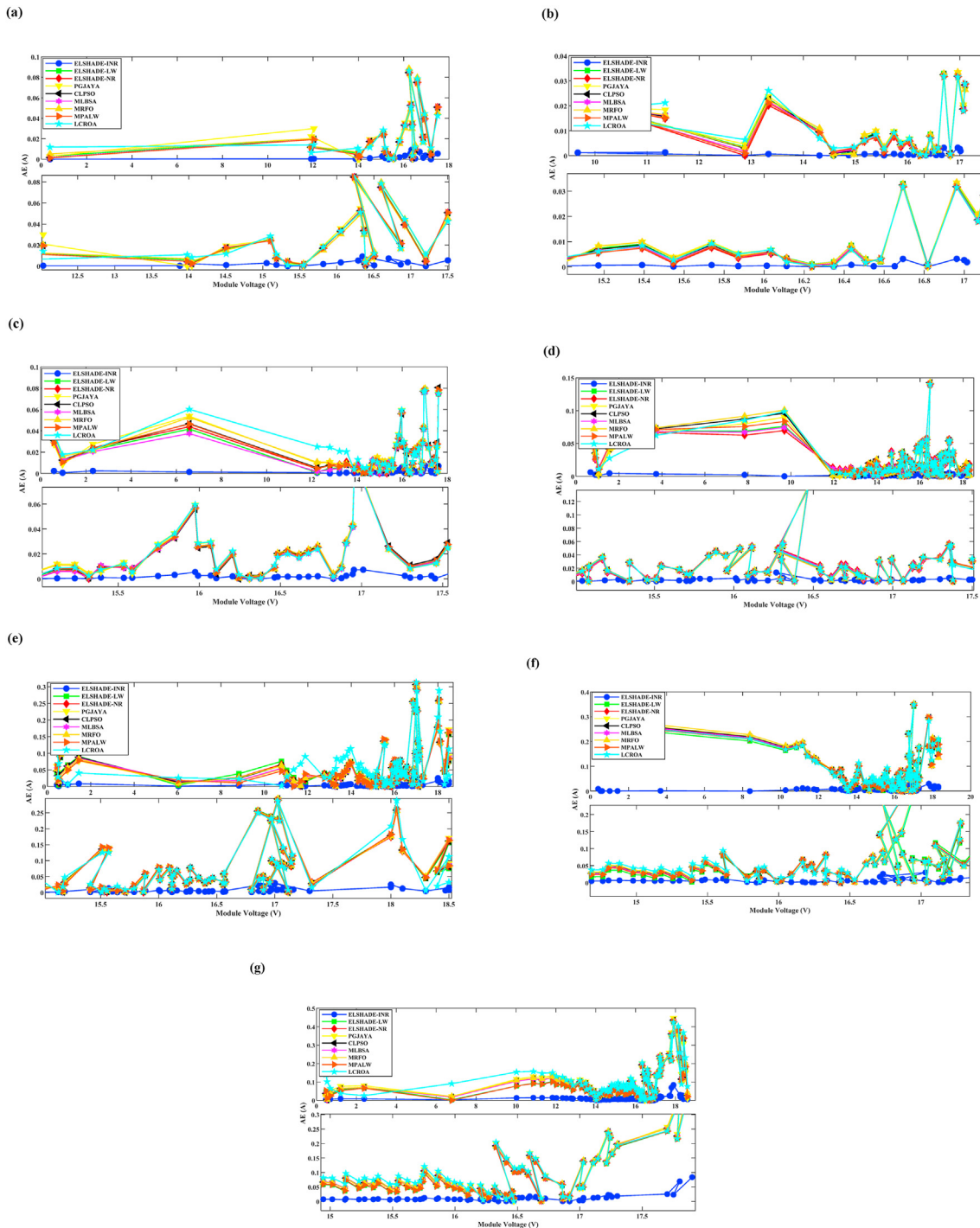


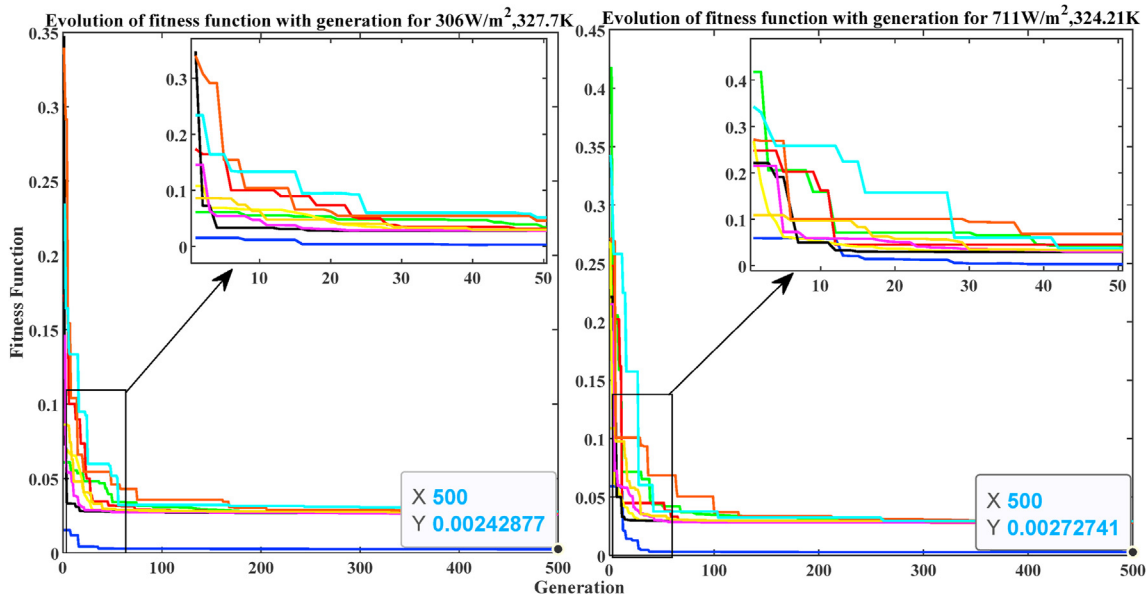
Fig. 8. AE with module voltage correlation under (S_1 - S_7) weather conditions (a-g).

of the proposed model. The ELSHADE-LW and MPALW share the second rank in term of average AE value with trivial superiority given to ELSHADE-LW method. This is because the Lambert W function has moderate converges except the high voltage ranges. While MLBSA is ranked the third method, followed by ELSHADE, CLPSO, PGJAYA, MRFO, and LCROA, respectively. According to Fig. 8, each level is plotted with actual and zoomed data to display the gap in the AE values clearly. Therefore, the proposed ELSHADE-INR approach provides very high-quality solutions for the nine parameter extraction PV model due to the effectively classified

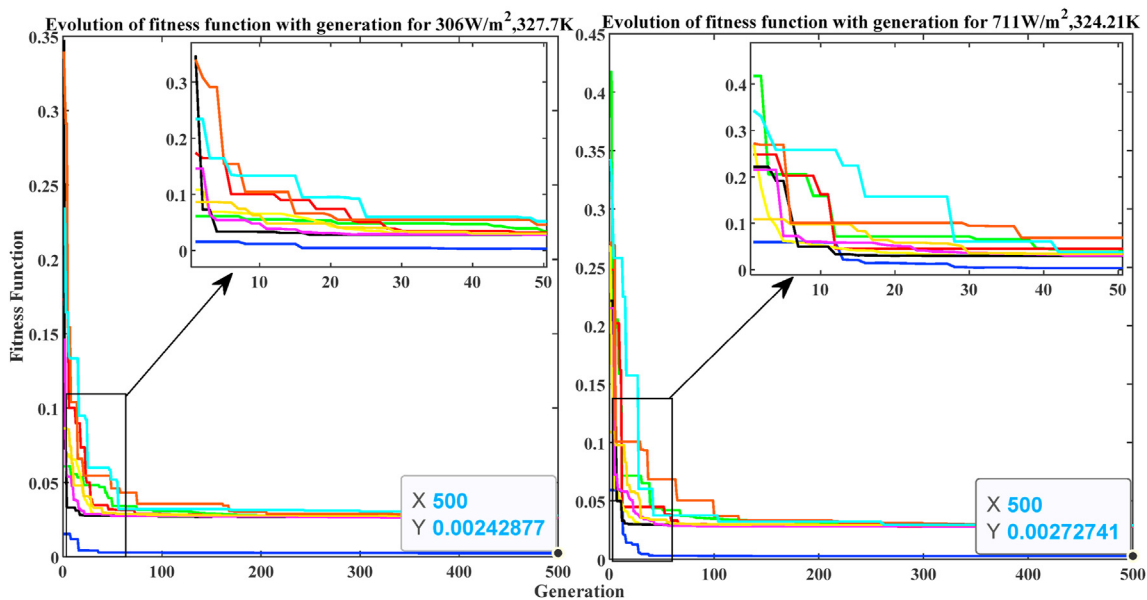
population on biases of the mutation and guided-chaotic strategies and profoundly discovering feature space.

The comparison has been vividly established to verify each method's convergence degree, as shown in Fig. 9. There is no doubt that the ELSHADE-INR has the highest and quickest convergence among all methods. It can be recognized that the ELSHADE-INR can almost convergence with 50 iterations, except for high levels of solar radiation. This is because of the high nonlinearity, multi-region valley, and increasing the number of the data points, which render the task is a challenging test to obtain minimum

(a-b)



(c-d)

**Fig. 9.** Comparison convergence of various methods under seven weather conditions (a–g).

RMSE value for these optimization algorithms.

In fact, few research studies consider the CPU runtime of the parameter extraction optimization problem. In this respect, a superiority time computation is achieved by the ELSHADE-INR method with an average CPU time of 11.39 (in seconds) compared with other optimizers, which has a minimum CPU time followed by the CLPSO method. At the same time, the worst is registered by the

MPALW method. Given that the ELSHADE-LW is ranked as a second method in terms of accuracy, it takes a very prolonged time since it calculates the currents in a deterministic way. This can confirm that the robustness, accuracy, reliability, convergence, and excellent CPU time of the proposed ELSHADE-INR method compared with well-published approaches as shown in Table 6. It can be affirmed that the improved NR method can efficiently select the initial root

values of the I–V curve equation in the next step, and therefore few iterations are required.

The proposed ELSHADE-INR approach can guarantee the TD PV model's global parameters in light of the above findings. This is attributed to the many main power points, such as the enhanced LSHADE method, by dividing the population into two parts. The first half of the population experienced a robust mutation scheme, while the second half was practicing a guided-chaotic technique. Therefore, the systematic equilibrium between exploitation and exploration phases has been achieved, but the convergence to the global solutions is boosted. Moreover, the improved NR method can significantly enhance the extracted parameters' quality, even at a complex model such as the TD PV model. Therefore, this study presents the novel ELSHADE-INR method. It has a minimum error, very high levels of accuracy and stability, little computational time,

and a quick convergence to optimal solutions that have been clearly shown by the above statistical results and compared with other well-published algorithms.

5. Conclusions and future directions

In this study, a novel version of the LSHADE method, named ELSHADE-INR, is proposed by integrating various algorithms' contributions and the objective function to extract the TD PV model parameters under real environmental conditions. The ELSHADE-INR is used to enrich the solution's diversity, fast convergence, and roughly estimate the TD PV equation's roots. The performance of the ELSHADE-INR is compared with two variants of the ELSHADE based on conventional NR and Lambert W function as well as well-published PGJAYA, CLPSO, MLBSA, MRFO, MPALW, and LCROA

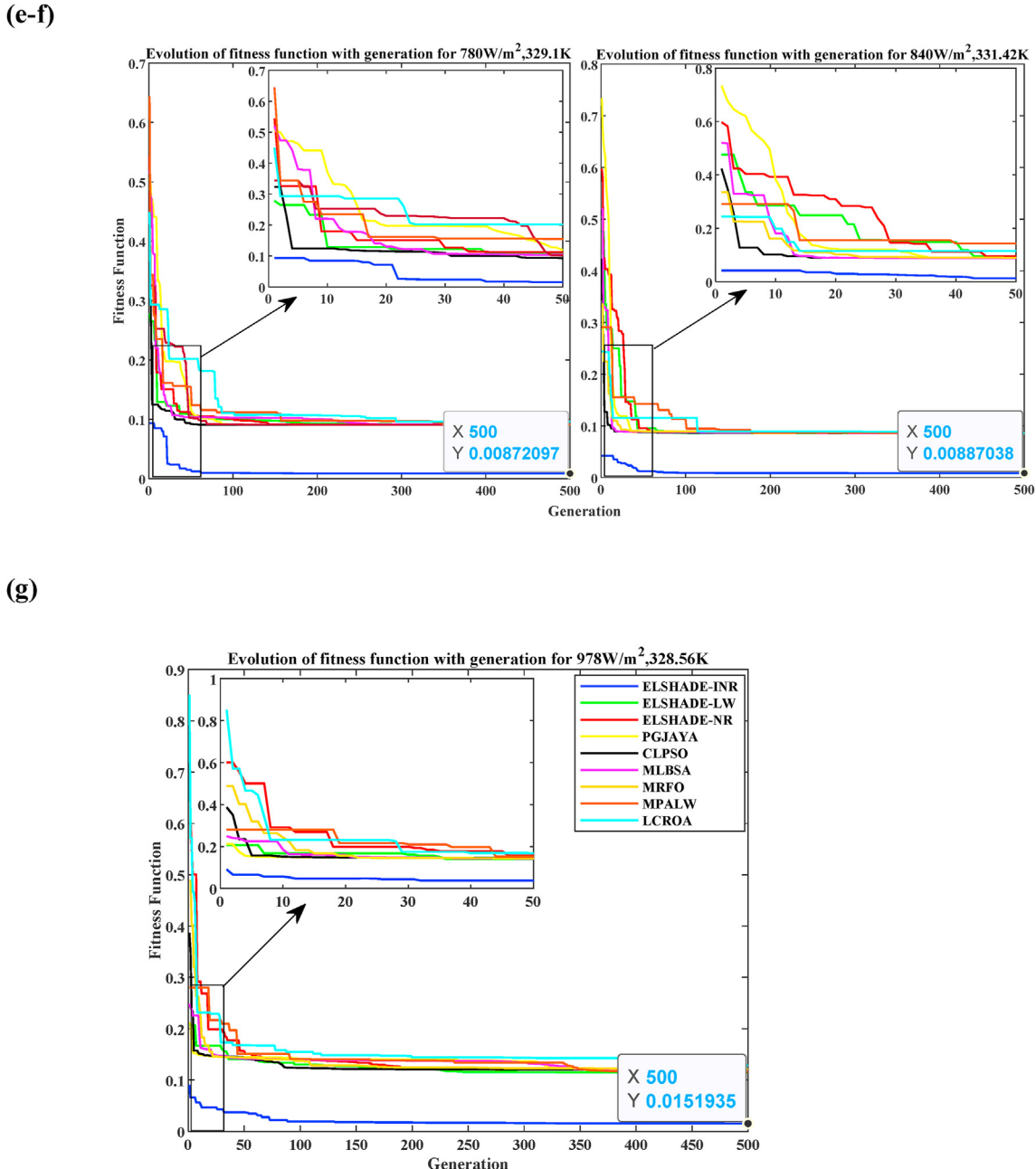


Fig. 9. (continued).

Table 6

CPU execution time.

CPU time	S_1	S_2	S_3	S_4	S_5	S_6	S_7	Avg.
ELSHADE-INR	10.32	10.68	10.68	11.98	11.67	12.17	12.21	11.39
ELSHADE-LW	145.50	322.00	1223.06	1475.42	1811.76	2138.85	2461.35	1368.28
ELSHADE	17.81	17.84	17.68	21.09	19.15	19.46	19.56	18.94
PGJAYA	14.84	15.40	16.40	19.60	16.14	17.89	17.07	16.76
CPSO	15.95	15.26	17.01	18.18	16.84	16.68	16.65	16.64
MLBSA	16.21	16.34	20.24	21.51	19.64	18.32	17.71	18.57
MRFO	33.23	22.20	27.03	26.90	27.10	32.14	26.84	27.92
MPALW	10153.95	5353.25	5161.48	582.68	3375.28	3633.75	3777.45	4576.83
LCROA	46.65	42.14	42.64	41.37	43.51	49.60	41.39	43.90

methods using real experimental data under seven weather conditions. The results of comparisons and evaluations prove the superiority of the ELSHADE-INR in terms of accuracy, stability, CPU execution time, and robustness. The experimental results and statistical criteria demonstrate that the ELSHADE-INR can early predict the TD PV model's optimal solutions even under rough weather conditions. Thus, the ELSHADE-INR is promising to be applied to extract the parameters of other PV modules.

For future directions, improving the objective function formulation by combining fast convergence of the NR with method has deeply deterministic measurement to reduce RMSE as much as possible to sufficiently reflect the PV model's actual performance. The proposed ELSHADE algorithm can also be applied to other domains such as prediction methods [115,116], deep learning [103–108], decision making [109–111], and energy systems [94–96], electric vehicle energy consumption [102] and energy prediction.

Credit author statement

Hussein Mohammed Ridha: Conceptualization, Methodology, Writing – Original Draft, Writing – Review & Editing, Software, Visualization, Investigation. **Hashim Hizam:** Conceptualization, Methodology, Formal Analysis, Investigation, Writing – Review & Editing, Funding Acquisition, Supervision. **Chandima Gomes:** Writing – Original Draft, Writing – Review & Editing, Software, Visualization, Investigation. **Ali Asghar Heidari:** Formal Analysis, Methodology, Writing – Review & Editing, Software, Visualization, Supervision. **Huiling Chen:** Conceptualization, Methodology, Formal Analysis, Investigation, Writing – Review & Editing, Funding Acquisition, Supervision. **Masoud Ahmadipour:** Writing – Review & Editing, Software, Visualization. **Dhiaa Halboot Muhsen:** Writing – Review & Editing, Software, Visualization. **Mokhalad Alghrairi:** Writing – Review & Editing, Software, Visualization.

Declaration of competing interest

The authors declare that there is no conflict of interests regarding the publication of article.

Appendix 1

Function [f] = fitness_function ($a1, a2, a3, Rs, Rp, Iph, Io1, Io2, Io3, G, Tc$)
 $Nsc = 36$; %Number of cells are connected in series per module
 $k = 1.3806503 \times 10^{-23}$; %Boltzmann constant (J/K)
 $q = 1.60217646 \times 10^{-19}$; %Electron charge in (Columb)
 $VT = (Nsc * k * Tc) / q$; %Diode thermal voltage (v)
%%%Reading the experimental voltage and current data%%%
load ('var_fitness_function_TD_LSHADE', 'Vp', 'le'); %%Computing the theoretical current%%
 $N = \text{length}(Vp)$;

```

Ip = zeros (size (Vp)); epsilon = 0.03; for h = 1:length (Vp)
F(h) = Iph-Io1*(exp ((Vp(h)+le(h)*Rs)/(a1*VT))-1)-Io2*(exp ((Vp(h)+le(h)*
Rs)/(a2*VT))-1)-Io3*(exp ((Vp(h)+le(h)*Rs)/(a3*VT))-1)-(Vp(h)+le(h)*Rs)/
Rp)-le(h); fd(h) = -(Io1*(Rs/a1*VT)*(exp ((Vp(h)+le(h)*Rs)/(a1*VT)))-(Io2*(Rs/a2*VT)*
(exp ((Vp(h)+le(h)*Rs)/(a2*VT)))-(Io3*(Rs/a3*VT)*(exp ((Vp(h)+le(h)*Rs)/(a3*VT)))-(Rs/Rp)-1; Ip(h) = le(h)-0.05*(F(h)/fd(h)); for i = 1:3
FF(h) = Iph-Io1*(exp ((Vp(h)+Ip(h)*Rs)/(a1*VT))-1)-Io2*(exp ((Vp(h)+Ip(h)*Rs)/(a2*VT))-1)-Io3*(exp ((Vp(h)+Ip(h)*Rs)/(a3*VT))-1)-(Vp(h)+Ip(h)*Rs)/
Rp)-Ip(h); fd(h) = -(Io1*(Rs/a1*VT)*(exp ((Vp(h)+Ip(h)*Rs)/(a1*VT)))-(Io2*(Rs/a2*VT)*
(exp ((Vp(h)+Ip(h)*Rs)/(a2*VT)))-(Io3*(Rs/a3*VT)*(exp ((Vp(h)+Ip(h)*Rs)/(a3*VT)))-(Rs/Rp)-1; Ip(h) = Ip(h)-0.05*(FF(h)/fd(h)); err(h) = abs (le(h)-Ip(h));
if err(h)<epsilon
break;
end
end
end
%%%Computing the fitness function%%
f = sqrt ((1/N)*sum ((le-Ip).^2));

```

References

- [1] Zhang R, Jiang T, Li F, Li G, Chen H, Li X. Coordinated bidding strategy of wind farms and power-to-gas facilities using a cooperative game approach. IEEE Trans Sustain Energy 2020;11:2545–55. <https://doi.org/10.1109/TSTE.2020.2965521>.
- [2] Wang B, Song Z, Sun L. A review: comparison of multi-air-pollutant removal by advanced oxidation processes – industrial implementation for catalytic oxidation processes. Chem Eng J 2021;409:128136. <https://doi.org/10.1016/j.cej.2020.128136>.
- [3] Orioli A, Di Gangi A. A procedure to calculate the five-parameter model of crystalline silicon photovoltaic modules on the basis of the tabular performance data. Appl Energy 2013;102:1160–77. <https://doi.org/10.1016/j.apenergy.2012.06.036>.
- [4] Hu X, Ma P, Gao B, Zhang M. An integrated step-up inverter without transformer and leakage current for grid-connected photovoltaic system. IEEE Trans Power Electron 2019;34:9814–27.
- [5] Perera ATD, Nik VM, Chen D, Scartezzini JL, Hong T. Quantifying the impacts of climate change and extreme climate events on energy systems. Nat Energy 2020;5:150–9. <https://doi.org/10.1038/s41560-020-0558-0>.
- [6] Ridha HM, Gomes C, Hizam H, Ahmadipour M. Sizing and implementing off-grid stand-alone photovoltaic/battery systems based on multi-objective optimization and techno-economic (MADE) analysis. Energy 2020;207:118163. <https://doi.org/10.1016/j.energy.2020.118163>.
- [7] Ridha HM, Gomes C, Hizam H, Ahmadipour M, Asghar Heidari A, Chen H. Multi-objective optimization and multi-criteria decision-making methods for optimal design of standalone photovoltaic system: a comprehensive review. Renew Sustain Energy Rev 2021;135:110202. <https://doi.org/10.1016/j.rser.2020.110202>.
- [8] Yu K, Qu B, Yue C, Ge S, Chen X, Liang J. A performance-guided JAYA algorithm for parameters identification of photovoltaic cell and module. Appl Energy 2019;237:241–57. <https://doi.org/10.1016/j.apenergy.2019.01.008>.
- [9] Ridha HM, Heidari AA, Wang M, Chen H. Boosted mutation-based Harris hawks optimizer for parameters identification of single-diode solar cell models. Energy Convers Manag 2020;209:112660. <https://doi.org/10.1016/j.enconman.2020.112660>.
- [10] Yang B, Wang J, Zhang X, Yu T, Yao W, Shu H, et al. Comprehensive overview of meta-heuristic algorithm applications on PV cell parameter identification.

- Energy Convers Manag 2020;208:112595. <https://doi.org/10.1016/j.enconman.2020.112595>.
- [11] Khanna V, Das BK, Bisht D, Vandana, Singh PK. A three diode model for industrial solar cells and estimation of solar cell parameters using PSO algorithm. Renew Energy 2015;78:105–13. <https://doi.org/10.1016/j.renene.2014.12.072>.
- [12] Ibrahim IA, Hossain MJ, Duck BC, Nadarajah M. An improved wind driven optimization algorithm for parameters identification of a triple-diode photovoltaic cell model. Energy Convers Manag 2020;213:112872. <https://doi.org/10.1016/j.enconman.2020.112872>.
- [13] Humada AM, Hojabri M, Mekhilef S, Hamada HM. Solar cell parameters extraction based on single and double-diode models: a review. Renew Sustain Energy Rev 2016;56:494–509. <https://doi.org/10.1016/j.rser.2015.11.051>.
- [14] Cardenas AA, Carrasco M, Mancilla-David F, Street A, Cardenas R. Experimental parameter extraction in the single-diode photovoltaic model via a reduced-space search. IEEE Trans Ind Electron 2017;64:1468–76. <https://doi.org/10.1109/TIE.2016.2615590>.
- [15] Chen H, Jiao S, Wang M, Heidari AA, Zhao X. Parameters identification of photovoltaic cells and modules using diversification-enriched Harris hawks optimization with chaotic drifts. J Clean Prod 2020;244:118778. <https://doi.org/10.1016/j.jclepro.2019.118778>.
- [16] Subudhi B, Pradhan R. Bacterial Foraging Optimization approach to parameter extraction of a photovoltaic module. IEEE Trans Sustain Energy 2018;9:381–9. <https://doi.org/10.1109/TSTE.2017.2736060>.
- [17] Easwarakhanth T, Bottin J, Bouhouche I, Boutrif C. Nonlinear minimization algorithm for determining the solar cell parameters with microcomputers. Int J Sol Energy 1986;4:1–12. <https://doi.org/10.1080/01425918608909835>.
- [18] Chan DSH, Phillips JR, Phang JCH. A comparative study of extraction methods for solar cell model parameters. Solid State Electron 1986;29:329–37. [https://doi.org/10.1016/0038-1101\(86\)90212-1](https://doi.org/10.1016/0038-1101(86)90212-1).
- [19] Ridha HM, Gomes C, Hizam H. Estimation of photovoltaic module model's parameters using an improved electromagnetic-like algorithm. Neural Comput Appl 2020;32:12627–42. <https://doi.org/10.1007/s00521-020-04714-z>.
- [20] Chaibi Y, Allouhi A, Salhi M. A simple iterative method to determine the electrical parameters of photovoltaic cell. J Clean Prod 2020;122363. <https://doi.org/10.1016/j.jclepro.2020.122363>.
- [21] Cotfas DT, Cotfas PA, Kaplanis S. Methods to determine the dc parameters of solar cells: a critical review. Renew Sustain Energy Rev 2013;28:588–96. <https://doi.org/10.1016/j.rser.2013.08.017>.
- [22] Yahya-Khotbehsara A, Shahhoseini A. A fast modeling of the double-diode model for PV modules using combined analytical and numerical approach. Sol Energy 2018;162:403–9. <https://doi.org/10.1016/j.solener.2018.01.047>.
- [23] Ghani F, Rosengarten G, Duke M, Carson JK. The numerical calculation of single-diode solar-cell modelling parameters. Renew Energy 2014;72:105–12. <https://doi.org/10.1016/j.renene.2014.06.035>.
- [24] Javier Toledo F, Blanes JM, Galiano V. Two-step linear least-squares method for photovoltaic single-diode model parameters extraction. IEEE Trans Ind Electron 2018;65:6301–8. <https://doi.org/10.1109/TIE.2018.2793216>.
- [25] Feblea DM, Bortoni EC, Oliveira AF, Rubinger RM. The effects of noises on metaheuristic algorithms applied to the PV parameter extraction problem. Sol Energy 2020;201:420–36. <https://doi.org/10.1016/j.solener.2020.02.093>.
- [26] Guerrero Delgado Mc, Sánchez Ramos J, Rodríguez Jara EA, Molina Félix JL, Álvarez Domínguez S. Decision-making approach: a simplified model for energy performance evaluation of photovoltaic modules. Energy Convers Manag 2018;177:350–62. <https://doi.org/10.1016/j.enconman.2018.09.080>.
- [27] Chenoard R, El-Sehiemy RA. An interval branch and bound global optimization algorithm for parameter estimation of three photovoltaic models. Energy Convers Manag 2020;205:112400. <https://doi.org/10.1016/j.enconman.2019.112400>.
- [28] Oulcaid M, El H, Ammeh L, Yahya A, Giri F. Parameter extraction of photovoltaic cell and module : analysis and discussion of various combinations and test cases. Sustain Energy Technol Assessments 2020;40:100736. <https://doi.org/10.1016/j.seta.2020.100736>.
- [29] Hejri M, Mokhtari H, Azizzian MR, Ghandhari M, Söder L. On the parameter extraction of a five-parameter double-diode model of photovoltaic cells and modules. IEEE J Photovoltaics 2014;4:915–23. <https://doi.org/10.1109/JPHOTOV.2014.2307161>.
- [30] Bliss M, Betts T, Gottschalg R, Salis E, Müllejans H, Winter S, et al. Inter-laboratory comparison of short-circuit current versus irradiance linearity measurements of photovoltaic devices. Sol Energy 2019;182:256–63. <https://doi.org/10.1016/j.solener.2019.02.031>.
- [31] Drouiche I, Harrouni S, Arab AH. A new approach for modelling the aging PV module upon experimental I–V curves by combining translation method and five-parameters model. Elec Power Syst Res 2018;163:231–41. <https://doi.org/10.1016/j.epsr.2018.06.014>.
- [32] Qu S, Han Y, Wu Z, Raza H. Consensus modeling with asymmetric cost based on data-driven robust optimization. Group Decis Negot 2020;1–38.
- [33] Fu X, Pace P, Aloisio G, Yang L, Fortino G. Topology optimization against cascading failures on wireless sensor networks using a memetic algorithm. Comput Network 2020;107327.
- [34] Cao B, Zhao J, Gu Y, Ling Y, Ma X. Applying graph-based differential grouping for multiobjective large-scale optimization. Swarm Evol Comput 2020;53:100626.
- [35] Liu J, Wu C, Wu G, Wang X. A novel differential search algorithm and applications for structure design. Appl Math Comput 2015;268:246–69.
- [36] Sun G, Yang B, Yang Z, Xu G. An adaptive differential evolution with combined strategy for global numerical optimization. Soft Comput 2019;1–20.
- [37] Bai B, Guo Z, Zhou C, Zhang W, Zhang J. Application of adaptive reliability importance sampling-based extended domain PSO on single mode failure in reliability engineering. Inf Sci 2021;546:42–59. <https://doi.org/10.1016/j.ins.2020.07.069>.
- [38] Gao N, Luo D, Cheng B, Hou H. Teaching-learning-based optimization of a composite metastructure in the 0–10 kHz broadband sound absorption range. J Acoust Soc Am 2020;148:EL125–E129.
- [39] Cao Y, Li Y, Zhang G, Jermsittiparsert K, Nasseri M. An efficient terminal voltage control for PEMFC based on an improved version of whale optimization algorithm. Energy Rep 2020;6:530–42.
- [40] Oliva D, Elaziz MA, Elsheikh AH, Ewees AA. A review on meta-heuristics methods for estimating parameters of solar cells. J Power Sources 2019;435:126683. <https://doi.org/10.1016/j.jpowsour.2019.05.089>.
- [41] Del Ser J, Osaba E, Molina D, Yang XS, Salcedo-Sanz S, Camacho D, et al. Bio-inspired computation: where we stand and what's next. Swarm Evol Comput 2019;48:220–50. <https://doi.org/10.1016/j.swevo.2019.04.008>.
- [42] Muhsen DH, Ghazali AB, Khatib T, Abed IA. A comparative study of evolutionary algorithms and adapting control parameters for estimating the parameters of a single-diode photovoltaic module's model. Renew Energy 2016;96:377–89. <https://doi.org/10.1016/j.renene.2016.04.072>.
- [43] Chin VJ, Salam Z, Ishaque K. Cell modelling and model parameters estimation techniques for photovoltaic simulator application: a review. Appl Energy 2015;154:500–19. <https://doi.org/10.1016/j.apenergy.2015.05.035>.
- [44] Oliva D, Cuevas E, Pajares G. Parameter identification of solar cells using artificial bee colony optimization. Energy 2014;72:93–102. <https://doi.org/10.1016/j.energy.2014.05.011>.
- [45] Ram JP, Babu TS, Dragicevic T, Rajasekar N. A new hybrid bee pollinator flower pollination algorithm for solar PV parameter estimation. Energy Convers Manag 2017;135:463–76. <https://doi.org/10.1016/j.enconman.2016.12.082>.
- [46] Nunes HGG, Pombo JAN, Bento PMR, Mariano SJPS, Calado MRA. Collaborative swarm intelligence to estimate PV parameters. Energy Convers Manag 2019;185:866–90. <https://doi.org/10.1016/j.enconman.2019.02.003>.
- [47] Muangkote N, Sunat K, Chiewchanwattana S, Kaiwinit S. An advanced onlooker-ranking-based adaptive differential evolution to extract the parameters of solar cell models. Renew Energy 2019;134:1129–47. <https://doi.org/10.1016/j.renene.2018.09.017>.
- [48] Biswas PP, Suganthan PN, Wu G, Amaralunga GAJ. Parameter estimation of solar cells using datasheet information with the application of an adaptive differential evolution algorithm. Renew Energy 2019;132:425–38. <https://doi.org/10.1016/j.renene.2018.07.152>.
- [49] Hao Q, Zhou Z, Wei Z, Chen G. Parameters identification of photovoltaic models using a multi-strategy success-history-based adaptive differential evolution. IEEE Access 2020;8:35979–94. <https://doi.org/10.1109/ACCESS.2020.2975078>.
- [50] Yu K, Liang JJ, Qu BY, Cheng Z, Wang H. Multiple learning backtracking search algorithm for estimating parameters of photovoltaic models. Appl Energy 2018;226:408–22. <https://doi.org/10.1016/j.apenergy.2018.06.010>.
- [51] Pillai DS, Rajasekar N. Metaheuristic algorithms for PV parameter identification: a comprehensive review with an application to threshold setting for fault detection in PV systems. Renew Sustain Energy Rev 2018;82:3503–25. <https://doi.org/10.1016/j.rser.2017.10.107>.
- [52] Gu W, Ma T, Ahmed S, Zhang Y, Peng J. A comprehensive review and outlook of bifacial photovoltaic (bpV) technology. Energy Convers Manag 2020;223. <https://doi.org/10.1016/j.enconman.2020.113283>.
- [53] Gnetchejo PJ, Ndjakoma Essiane S, Ele P, Wamkeue R, Mbadjoun Wapet D, Perabi Ngoffe S. Important notes on parameter estimation of solar photovoltaic cell. Energy Convers Manag 2019;197:111870. <https://doi.org/10.1016/j.enconman.2019.111870>.
- [54] Lun SX, Du CJ, Guo TT, Wang S, Sang JS, Li JP. A new explicit i-v model of a solar cell based on taylor's series expansion. Sol Energy 2013;94:221–32. <https://doi.org/10.1016/j.solener.2013.04.013>.
- [55] Jordehi AR. Time varying acceleration coefficients particle swarm optimisation (TVACPSO): a new optimisation algorithm for estimating parameters of PV cells and modules. Energy Convers Manag 2016;129:262–74. <https://doi.org/10.1016/j.enconman.2016.09.085>.
- [56] Villalva MG, Gazoli JR, Filho ER. Comprehensive approach to modeling and simulation of photovoltaic arrays. IEEE Trans Power Electron 2009;24:1198–208. <https://doi.org/10.1109/TPEL.2009.2013862>.
- [57] Gao X, Cui Y, Hu J, Xu G, Yu Y, Lambert W-function based exact representation for double diode model of solar cells: comparison on fitness and parameter extraction. Energy Convers Manag 2016;127:443–60. <https://doi.org/10.1016/j.enconman.2016.09.005>.
- [58] Čalasan M, Abdel Aleem SHE, Zobaia AF. On the root mean square error (RMSE) calculation for parameter estimation of photovoltaic models: a novel exact analytical solution based on Lambert W function. Energy Convers Manag 2020;210:112716. <https://doi.org/10.1016/j.enconman.2020.112716>.
- [59] Chen Y, Sun Y, Meng Z. An improved explicit double-diode model of solar cells: fitness verification and parameter extraction. Energy Convers Manag 2018;169:345–58. <https://doi.org/10.1016/j.enconman.2018.05.035>.
- [60] Kalantari B. Generalization of Taylor's theorem and Newton's method via a

- new family of determinantal interpolation formulas and its applications. *J. Comput. Appl. Math.* 2000;126:287–318. [https://doi.org/10.1016/S0377-0427\(99\)00360-X](https://doi.org/10.1016/S0377-0427(99)00360-X).
- [61] Yousri D, Abd Elaziz M, Oliva D, Abualigah L, Al-qaness MAA, Ewees AA. Reliable applied objective for identifying simple and detailed photovoltaic models using modern metaheuristics: comparative study. *Energy Convers. Manag.* 2020;223:113279. <https://doi.org/10.1016/j.enconman.2020.113279>.
- [62] Das S, Suganthan PN. Differential evolution: a survey of the state-of-the-art. *IEEE Trans. Evol. Comput.* 2011;15:4–31. <https://doi.org/10.1109/TEVC.2010.2059031>.
- [63] Das S, Mullick SS, Suganthan PN. Recent advances in differential evolution: An updated survey. *Swarm Evol. Comput.* 2016;27:1–30. <https://doi.org/10.1016/j.swevo.2016.01.004>.
- [64] Bilal Pant M, Zaheer H, Garcia-Hernandez L, Abraham A. Differential Evolution: a review of more than two decades of research. *Eng. Appl. Artif. Intell.* 2020;90:103479. <https://doi.org/10.1016/j.engappai.2020.103479>.
- [65] Yang X, Gong W, Wang L. Comparative study on parameter extraction of photovoltaic models via differential evolution. *Energy Convers. Manag.* 2019;201:112113. <https://doi.org/10.1016/j.enconman.2019.112113>.
- [66] Lekouaghet B, Boukabou A, Boubakir C. Estimation of the photovoltaic cells/modules parameters using an improved Rao-based chaotic optimization technique. *Energy Convers. Manag.* 2021;229:113722. <https://doi.org/10.1016/j.enconman.2020.113722>.
- [67] Ridha HM. Parameters extraction of single and double diodes photovoltaic models using Marine Predators Algorithm and Lambert W function. *Sol. Energy* 2020;209:674–93. <https://doi.org/10.1016/j.solener.2020.09.047>.
- [68] El-Hameed MA, Elkholly MM, El-Fergany AA. Three-diode model for characterization of industrial solar generating units using Manta-rays foraging optimizer: analysis and validations. *Energy Convers. Manag.* 2020;219:113048. <https://doi.org/10.1016/j.enconman.2020.113048>.
- [69] Tossa AK, Soro YM, Azoumah Y, Yamgueu D. A new approach to estimate the performance and energy productivity of photovoltaic modules in real operating conditions. *Sol. Energy* 2014;110:543–60. <https://doi.org/10.1016/j.solener.2014.09.043>.
- [70] Muhsen DH, Ghazali AB, Khatib T, Abed IA. Parameters extraction of double diode photovoltaic module's model based on hybrid evolutionary algorithm. *Energy Convers. Manag.* 2015;105:552–61. <https://doi.org/10.1016/j.enconman.2015.08.023>.
- [71] Abbassi A, Gammoudi R, Ali Dami M, Hasnaoui O, Jemli M. An improved single-diode model parameters extraction at different operating conditions with a view to modeling a photovoltaic generator: a comparative study. *Sol. Energy* 2017;155:478–89. <https://doi.org/10.1016/j.solener.2017.06.057>.
- [72] Elbaset AA, Ali H, Abd-El Sattar M. Novel seven-parameter model for photovoltaic modules. *Sol. Energy Mater. Sol. Cells* 2014;130:442–55. <https://doi.org/10.1016/j.solmat.2014.07.016>.
- [73] Nassar-Eddine I, Obbadi A, Errami Y, El Fajri A, Agounou M. Parameter estimation of photovoltaic modules using iterative method and the Lambert W function: a comparative study. *Energy Convers. Manag.* 2016;119:37–48. <https://doi.org/10.1016/j.enconman.2016.04.030>.
- [74] Crisfield MA. Accelerating and damping the modified Newton-Raphson method. *Comput. Struct.* 1984;18:395–407. [https://doi.org/10.1016/0045-7949\(84\)90059-2](https://doi.org/10.1016/0045-7949(84)90059-2).
- [75] Appelbaum J, Peled A. Parameters extraction of solar cells - a comparative examination of three methods. *Sol. Energy Mater. Sol. Cells* 2014;122:164–73. <https://doi.org/10.1016/j.solmat.2013.11.011>.
- [76] Amrein M, Wihler TP. An adaptive Newton-method based on a dynamical systems approach. *Commun. Nonlinear Sci. Numer. Simulat.* 2014;19:2958–73. <https://doi.org/10.1016/j.cnsns.2014.02.010>.
- [77] McDougall TJ, Wotherspoon SJ. A simple modification of Newton's method to achieve convergence of order $1 + \sqrt{2}$. *Appl. Math. Lett.* 2014;29:20–5. <https://doi.org/10.1016/j.aml.2013.10.008>.
- [78] Storn R, Price K. Differential evolution – a simple and efficient heuristic for global optimization over continuous spaces. *J. Global Optim.* 1997;11:341–59. <https://doi.org/10.1023/A:1008202821328>.
- [79] Tanabe R, Fukunaga AS. Improving the search performance of SHADE using linear population size reduction. *Proc. 2014 IEEE Congr. Evol. Comput. CEC 2014* 2014:1658. <https://doi.org/10.1109/CEC.2014.6900380>.
- [80] Tanabe R, Fukunaga A. Success-history based parameter adaptation for Differential Evolution. *IEEE Congr. Evol. Comput. CEC 2013*:71. <https://doi.org/10.1109/CEC2013.6557555>.
- [81] Mohamed AW, Hadi AA, Jambi KM. Novel mutation strategy for enhancing SHADE and LSHADE algorithms for global numerical optimization. *Swarm Evol. Comput.* 2019;50. <https://doi.org/10.1016/j.swevo.2018.10.006>.
- [82] Al-Dabbagh RD, Neri F, Idris N, Baba MS. Algorithmic design issues in adaptive differential evolution schemes: review and taxonomy. *Swarm Evol. Comput.* 2018;43:284–311. <https://doi.org/10.1016/j.swevo.2018.03.008>.
- [83] Shi K, Tang Y, Liu X, Zhong S. Non-fragile sampled-data robust synchronization of uncertain delayed chaotic Lurie systems with randomly occurring controller gain fluctuation. *ISA Trans.* 2017;66:185–99.
- [84] Liang JJ, Qin AK, Member S, Suganthan PN, Member S, Baskar S. Comprehensive learning particle swarm optimizer for global optimization of multimodal functions. *IEEE Trans. Evol. Comput.* 2006;10:281–95.
- [85] Muhsen DH, Ghazali AB, Khatib T, Abed IA. Extraction of photovoltaic module's parameters using an improved hybrid differential evolution/electromagnetism-like algorithm. *Sol. Energy* 2015;119:286–97. <https://doi.org/10.1016/j.solener.2015.07.008>.
- [86] Steingrube S, Breitenstein O, Ramspeck K, Glunz S, Schenk A, Altermatt PP. Explanation of commonly observed shunt currents in c-Si solar cells by means of recombination statistics beyond the Shockley-Read-Hall approximation. *J. Appl. Phys.* 2011;110. <https://doi.org/10.1063/1.3607310>.
- [87] Khatibi A, Razi Astaraei F, Ahmad M. Generation and combination of the solar cells: a current model review. *Energy Sci. Eng.* 2019;7:305–22. <https://doi.org/10.1002/ese3.292>.
- [88] Ridha M H, Gomes C, Hizam H, Ahmadipour M, Muhsen Halboot D, Ethaib S. Optimum design of a standalone solar photovoltaic system based on novel integration of iterative-PESA-II and AHP-VIKOR methods. *Processes* 2020;8(3):1–23. <https://doi.org/10.3390/pr8030367>.
- [89] Wang B, Zhang L, Ma H, Wang H, Wan S. Parallel LSTM-based regional integrated energy system multienergy source-load information interactive energy prediction. *Complexity* 2019. <https://doi.org/10.1155/2019/7414318>.
- [90] Chen Y, He L, Guan Y, Lu H, Li J. Life cycle assessment of greenhouse gas emissions and water-energy optimization for shale gas supply chain planning based on multi-level approach: Case study in Barnett, Marcellus, Fayetteville, and Haynesville shales. *Energy Convers. Manag.* 2017;134:382–98.
- [91] Lu H, Tian P, He L. Evaluating the global potential of aquifer thermal energy storage and determining the potential worldwide hotspots driven by socio-economic, geo-hydrologic and climatic conditions. *Renew. Sustain. Energy Rev.* 2019;112:788–96.
- [92] Lu H, Guan Y, He L, Adhikari H, Pellikka P, Heiskanen J, et al. Patch aggregation trends of the global climate landscape under future global warming scenario. *Int. J. Climatol.* 2020;40(5):2674–85.
- [93] Wang B, Song Z, Sun L. A review: Comparison of multi-air-pollutant removal by advanced oxidation processes—Industrial implementation for catalytic oxidation processes. *Chem. Eng. J.* 2020;409:128136.
- [94] Zuo X, Dong M, Gao F, Tian S. The modeling of the electric heating and cooling system of the integrated energy system in the coastal area. *J. Coast. Res.* 2020;103(SI):1022–9.
- [95] Yang C, Gao F, Dong M. Energy efficiency modeling of integrated energy system in coastal areas. *J. Coast. Res.* 2020;103(SI):995–1001.
- [96] Yu D, Mao Y, Gu B, Nojavan S, Jermitsiparsert K, Nasseri M. A new LQG optimal control strategy applied on a hybrid wind turbine/solid oxide fuel cell/in the presence of the interval uncertainties. *Sustain. Energy Grids Networks* 2020;21:100296.
- [97] Cao B, Zhao J, Yang P, Gu Y, Muhammad K, Rodrigues JJ, et al. Multiobjective 3-D topology optimization of next-generation wireless data center network. *IEEE Trans. Ind. Inf.* 2019;16(5):3597–605.
- [98] Cao B, Dong W, Lv Z, Gu Y, Singh S, Kumar P. Hybrid microgrid many-objective sizing optimization with fuzzy decision. *IEEE Trans. Fuzzy Syst.* 2020;28(11):2702–10.
- [99] Cao B, Wang X, Zhang W, Song H, Lv Z. A many-objective optimization model of industrial internet of things based on private blockchain. *IEEE Network* 2020;34(5):78–83.
- [100] Chen H, Qiao H, Xu L, Feng Q, Cai K. A fuzzy optimization strategy for the implementation of RBF-LSSVR model in vis-NIR analysis of pomelo maturity. *IEEE Trans. Ind. Inf.* 2019;15(11):5971–9.
- [101] Sun G, Li C, Deng L. An adaptive regeneration framework based on search space adjustment for differential evolution. *Neural Comput. & Applic.* 2021. <https://doi.org/10.1007/s00521-021-05708-1>.
- [102] Zhao X, Ye Y, Ma J, Shi P, Chen H. Construction of electric vehicle driving cycle for studying electric vehicle energy consumption and equivalent emissions. *Environ. Sci. Pollut. Res.* 2020;27(30):37395–409.
- [103] Chen H, Chen A, Xu L, Xie H, Qiao H, Lin Q, et al. A deep learning CNN architecture applied in smart near-infrared analysis of water pollution for agricultural irrigation resources. *Agric. Water Manag.* 2020;240:106303.
- [104] Qian J, Feng S, Li Y, Tao T, Han J, Chen Q, et al. Single-shot absolute 3D shape measurement with deep-learning-based color fringe projection profilometry. *Opt. Lett.* 2020;45(7):1842–5.
- [105] Li T, Xu M, Zhu C, Yang R, Wang Z, Guan Z. A deep learning approach for multi-frame in-loop filter of HEVC. *IEEE Trans. Image Process.* 2019;28(11):5663–78.
- [106] Xu M, Li T, Wang Z, Deng X, Yang R, Guan Z. Reducing complexity of HEVC: A deep learning approach. *IEEE Trans. Image Process.* 2018;27(10):5044–59.
- [107] Qiu T, Shi X, Wang J, Li Y, Qu S, Cheng Q, et al. Deep learning: a rapid and efficient route to automatic metasurface design. *Adv. Sci.* 2019;6(12):1900128.
- [108] Qian J, Feng S, Tao T, Hu Y, Li Y, Chen Q, et al. Deep-learning-enabled geometric constraints and phase unwrapping for single-shot absolute 3d shape measurement. *APL Photonics* 2020;5(4):046105.
- [109] Liu S, Chan FT, Ran W. Decision making for the selection of cloud vendor: An improved approach under group decision-making with integrated weights and objective/subjective attributes. *Expert Syst. Appl.* 2016;55:37–47.
- [110] Wu C, Wu P, Wang J, Jiang R, Chen M, Wang X. Critical review of data-driven decision-making in bridge operation and maintenance. *Struct. Infrastruct. Eng.*

- 2020:1–24. <https://doi.org/10.1080/15732479.2020.1833946>.
- [111] Liu S, Yu W, Chan FT, Niu B. A variable weight-based hybrid approach for multi-attribute group decision making under interval-valued intuitionistic fuzzy sets. *Int J Intell Syst* 2021;36(2):1015–52.
- [112] Shi K, Tang Y, Zhong S, Yin C, Huang X, Wang W. Nonfragile asynchronous control for uncertain chaotic Lurie network systems with Bernoulli stochastic process. *Int J Robust Nonlinear Control* 2018;28(5):1693–714.
- [113] Wu T, Cao J, Xiong L, Zhang H. New stabilization results for semi-Markov chaotic systems with fuzzy sampled-data control. *Complexity* 2019;2019.
- <https://doi.org/10.1155/2019/7875305>.
- [114] Wang B, Zhang BF, Liu XW. An image encryption approach on the basis of a time delay chaotic system. *Optik* 2021;225:165737.
- [115] Qu K, Wei L, Zou Q. A review of DNA-binding proteins prediction methods. *Curr Bioinf* 2019;14(3):246–54.
- [116] Jiang Q, Wang G, Jin S, Li Y, Wang Y. Predicting human microRNA-disease associations based on support vector machine. *Int J Data Min Bioinf* 2013;8(3):282–93.